



1 **On the Relationship Between Cloud Water Composition and Cloud Droplet Number**
2 **Concentration**

3
4 Alexander B. MacDonald¹, Ali Hossein Mardi¹, Hossein Dadashazar¹, Mojtaba Azadi Aghdam¹,
5 Ewan Crosbie^{2,3}, Haflidi H. Jonsson⁴, Richard C. Flagan⁵, John H. Seinfeld⁵, Armin
6 Sorooshian^{1,6*}

7
8 ¹Department of Chemical and Environmental Engineering, University of Arizona, Tucson, AZ,
9 USA

10 ²Science Systems and Applications, Inc., Hampton, VA, USA

11 ³NASA Langley Research Center, Hampton, VA, USA

12 ⁴Naval Postgraduate School, Monterey, CA, USA

13 ⁵Department of Chemical Engineering, California Institute of Technology, Pasadena, CA, USA

14 ⁶Department of Hydrology and Atmospheric Sciences, University of Arizona, Tucson, AZ, USA

15

16 *Corresponding author: armin@email.arizona.edu



17 **Abstract**

18 Aerosol-cloud interactions are the largest source of uncertainty in quantifying
19 anthropogenic radiative forcing. The large uncertainty is, in part, due to the difficulty of
20 predicting cloud microphysical parameters, such as the cloud droplet number concentration (N_d).
21 Even though rigorous first-principle approaches exist to calculate N_d , the cloud and aerosol
22 research community also relies on empirical approaches such as relating N_d to aerosol mass
23 concentration. Here we analyze relationships between N_d and cloud water chemical composition,
24 in addition to the effect of environmental factors on the degree of the relationships. Warm,
25 marine, stratocumulus clouds off the California coast were sampled throughout four summer
26 campaigns between 2011 and 2016. A total of 385 cloud water samples were collected and
27 analyzed for 79 chemical species. Single- and multi-species log-log linear regressions were
28 performed to predict N_d using chemical composition. Single-species regressions reveal that the
29 species that best predicts N_d is total sulfate ($R^2_{adj} = 0.40$). Multi-species regressions reveal that
30 adding more species does not necessarily produce a better model, as six or more species yield
31 regressions that are statistically insignificant. A commonality among the multi-species
32 regressions that produce the highest correlation with N_d was that most included sulfate (either
33 total or non-sea salt), an ocean emissions tracer (such as sodium), and an organic tracer (such as
34 oxalate). Binning the data according to turbulence, smoke influence, and in-cloud height allowed
35 examination of the effect of these environmental factors on the composition- N_d correlation.
36 Accounting for turbulence, quantified as the standard deviation of vertical wind speed, showed
37 that the correlation between N_d with both total sulfate and sodium increased at higher turbulence
38 conditions, consistent with turbulence promoting the mixing between ocean surface and cloud
39 base. Considering the influence of smoke significantly improved the correlation with N_d for two
40 biomass burning tracer species in the study region, specifically oxalate and iron. When binning
41 by in-cloud height, non-sea salt sulfate and sodium correlated best with N_d at cloud top, whereas
42 iron and oxalate correlate best with N_d at cloud base.

43
44
45
46



47 1. Introduction

48 To assess the degree to which humans have altered Earth's climate, it is necessary to
49 quantify the effect that particles in the air (i.e., aerosols) have on clouds. Some fraction of
50 aerosols (called cloud condensation nuclei, CCN) activate into cloud droplets, thus impacting the
51 cloud droplet number concentration (N_d). For warm marine boundary layer (MBL) clouds at
52 fixed liquid water, higher N_d values result in (i) higher cloud albedo (thus cooling the Earth and
53 counteracting the greenhouse effect) (Twomey, 1977), and (ii) delayed and/or reduced
54 precipitation (Albrecht, 1989). The complex interactions and feedback mechanisms between
55 aerosols, meteorology, and clouds leads to aerosol-cloud interactions as the largest source of
56 uncertainty in climate models (IPCC, 2013).

57 It is indispensable to know the value of N_d , but this is a difficult parameter to accurately
58 simulate and retrieve (Fountoukis & Nenes, 2005). There is a need to improve N_d retrievals from
59 satellite remote sensors, which provide broad spatial and temporal coverage in contrast to surface
60 sites and airborne research flights. Currently, N_d retrievals are limited to inferred values based on
61 values of cloud optical depth, cloud droplet effective radius, and temperature, along with
62 assumptions such as vertical homogeneity of N_d and monotonic increases in liquid water content
63 at a constant fraction of its adiabatic value (Grosvenor et al., 2018). Ultimately, measurements
64 are needed to better inform climate models about the cloud droplet activation process and better
65 constraining N_d values. Current general circulation models (GCMs) calculate N_d using the
66 properties of aerosol particles in one of two ways (Ghan et al., 1997; Menon et al., 2002). First,
67 there is a rigorous approach that is based on physical principles that predicts N_d based on aerosol
68 properties and meteorological conditions (Abdul-Razzak & Ghan, 2000). Second, there is an
69 empirical approach that parameterizes N_d using either the number concentration of aerosols, N_a
70 [$\# \text{ cm}^{-3}$], the number concentration of CCN, N_{CCN} [$\# \text{ cm}^{-3}$], or the mass concentration of chemical
71 species that comprise the aerosols (Ghan et al., 1997).

72 The rigorous approach predicts N_d by considering aerosol properties (e.g., size
73 distribution and chemical composition), microphysical processes (e.g., the seeding of cloud
74 droplets by particles, droplet growth, and droplet evaporation), and meteorological parameters
75 (e.g., relative humidity and the vertical updraft velocity transporting aerosols to cloud base) (e.g.,
76 Chuang et al., 1992; Chuang & Penner, 1995; Nenes & Seinfeld, 2003; Partridge et al., 2012).
77 This method is based on the physical principle that an aerosol particle needs to be a CCN in
78 order to seed a cloud droplet; consequently, the input for this approach is N_a , from which to
79 calculate N_{CCN} , and subsequently N_d . The requisite information for these calculations may not be
80 readily available for GCMs. A limitation is that the spatial resolution of a GCM may be too
81 coarse to capture the small-scale spatial variation of updraft velocity (Ghan et al., 2011; West et
82 al., 2014).

83 The empirical parameterization approach of interest in the present study uses the mass
84 concentration of one or several chemical species and correlates it/them directly to N_{CCN} or N_d .
85 Aerosols containing the sulfate ion (SO_4^{2-}) have long been known to serve as effective CCN
86 (Andreae & Rosenfeld, 2008; Charlson et al., 1992; Lance et al., 2009; Medina et al., 2007).
87 Sulfate is both contained in sea salt and is a product of the oxidation of gaseous sulfur dioxide
88 (SO_2) (Hegg et al., 1981; Quinn et al., 2017), so it is customary to isolate the anthropogenic
89 contribution to total SO_4^{2-} by considering its non-sea salt fraction (NSS- SO_4^{2-}). Therefore, most
90 studies choose either total SO_4^{2-} (denoted hereafter as Tot- SO_4^{2-}) or NSS- SO_4^{2-} to predict N_{CCN}
91 and N_d (e.g., Leaitch et al., 1992; Novakov et al., 1994; Saxena & Menon, 1999). Using the mass
92 concentration of SO_4^{2-} or any other chemical species to predict N_d : (i) circumvents the complex



93 intermediate microphysical steps to go from an aerosol particle to a cloud droplet and implicitly
94 accounts for such meteorological variables like updraft velocity, (ii) is based on actual
95 measurements, and (iii) can be compared directly to the mass concentration of different species
96 produced by aerosol transport models (e.g., Boucher & Lohmann, 1995; Chen & Penner, 2005).
97 The limitations of using an empirical parameterization are: (i) assuming a mass size distribution
98 of the aerosols, (ii) assuming that one or a few chemical species are responsible for all CCN, and
99 (iii) uncertainty in generalizing field data from one region (or a few regions) under specific
100 conditions to the entire globe for all conditions (Pringle et al., 2009). Despite these drawbacks,
101 empirical correlations of N_d and the mass concentration of different species are valuable. For
102 example, of the 20 studies addressing the cloud albedo effect considered in the IPCC Fourth
103 Assessment Report (IPCC, 2007), half relied on empirical relationships to calculate N_d (Pringle
104 et al., 2009).

105 Several studies have developed empirical correlations between N_{CCN} and the mass
106 concentration of SO_4^{2-} (e.g., Adams & Seinfeld, 2003; Hegg et al., 1993; Matsumoto et al.,
107 1997). However, the present objective is to focus on improving the prediction of N_d , not N_{CCN} ,
108 using the mass concentration of SO_4^{2-} in addition to other species. A log-log relation is often
109 used to correlate the mass concentration of SO_4^{2-} to N_d with an equation of the form (e.g.,
110 Lowenthal et al., 2004):

$$111 \log(N_d) = a_0 + a_1 \log([\text{SO}_4^{2-}]) \quad (1)$$

112 where $[\text{SO}_4^{2-}]$ is the mass concentration in air [$\mu\text{g m}^{-3}$], and a_0 and a_1 are fitting parameters. A
113 log-log relation is chosen to accommodate large ranges in N_d and SO_4^{2-} and to reduce sensitivity
114 of results to the measurement accuracy of each individual parameter (Boucher & Lohmann,
115 1995). The mass concentration of SO_4^{2-} can be obtained by analyzing either aerosol particles or
116 cloud water. When analyzing cloud water, the mass concentration of SO_4^{2-} dissolved in droplets
117 [mg lit^{-1}] is converted to the air-equivalent mass concentration [$\mu\text{g m}^{-3}$] by multiplying by the
118 liquid water content, LWC [g m^{-3}], in a cloud. The data used to create N_d - SO_4^{2-} empirical
119 parameterizations are typically derived from field campaigns, which differ in the region of
120 analysis, sampling platforms (aircraft or ground-based), measurement approach (e.g., in particle
121 form or dissolved in cloud water), and number of species analyzed. While the literature
122 evaluating relationships between cloud water composition and N_d is limited and largely from
123 aircraft studies from more than a decade ago, there is a growing number of datasets
124 characterizing N_d and cloud water composition that are of interest to continue this line of
125 research. Examples include the recently completed Cloud, Aerosol, and Monsoon Processes
126 Philippines Experiment (CAMP²Ex) and the North Atlantic Aerosols and Marine Ecosystems Study
127 (NAAMES) (Behrenfeld et al., 2019), and the current multi-year Aerosol Cloud meTeorology
128 Interactions oVer the western ATLantic Experiment (ACTIVATE) (Sorooshian et al., 2020). A
129 summary of relevant past field work follows.

130 Leaitch et al. (1986) sampled stratiform and cumuliform clouds over Ontario, Canada and
131 showed a roughly linear relationship between N_d and SO_4^{2-} at low SO_4^{2-} concentrations (below ~
132 $5 \mu\text{g m}^{-3}$), and that the relationship leveled out at higher concentration (Novakov et al., 1994).
133 Leaitch et al. (1992) suggested that the low R^2 values for the linear regression between N_d and
134 SO_4^{2-} for both stratiform and cumuliform clouds (0.30 and 0.49, respectively) stemmed from
135 factors such as (i) other chemical species besides SO_4^{2-} , and variability in both (ii) updraft wind
136 speed and (iii) temperature. Pueschel et al. (1986) sampled clouds originating from marine and
137
138



139 continental air masses at a ground-based observatory at Whiteface Mountain, New York. They
140 found that emissions contributed strongly to SO_4^{2-} , and that a significant portion of SO_4^{2-} -
141 containing particles acted as CCN, and thus likely impacted N_d . Novakov et al. (1994) sampled
142 marine cumulus and stratocumulus clouds by El Yunque peak in Puerto Rico. Although they
143 showed that N_{CCN} and SO_4^{2-} were highly correlated in both cumulus and stratocumulus clouds,
144 they also found that N_d and SO_4^{2-} were weakly correlated for stratocumulus clouds, and not
145 correlated for cumulus clouds. They attributed this difference to the effect of entrainment and
146 mixing on cloud microphysics. Leaitch et al. (1996) sampled marine stratus clouds over the Gulf
147 of Maine and the Bay of Fundy during the North Atlantic Regional Experiment (NARE) and
148 showed that SO_4^{2-} was better correlated with N_d than nitrate (NO_3^-) (with an R^2 of 0.30 and 0.12,
149 respectively). The R^2 between N_d and SO_4^{2-} increased when the data were stratified into bins of
150 low and high turbulence, which was quantified as the standard deviation of vertical wind speed.
151 They found that in situations with lower supersaturations, N_d was more influenced by turbulence
152 than by either SO_4^{2-} or N_a . Menon & Saxena (1998) and Saxena & Menon (1999) sampled
153 orographic clouds at a ground-based station at Mt. Mitchell, North Carolina. They found that
154 SO_4^{2-} was the main contributor to cloud water acidity and a reliable tracer for anthropogenic
155 pollution. Log-log regressions of SO_4^{2-} - N_d were binned according to the level of SO_4^{2-} , with not
156 much difference observed between the different levels of pollution. Borys et al. (1998) and
157 Lowenthal & Borys (2000) sampled warm marine stratiform clouds on the Island of Tenerife in
158 the Canary Islands. They found that N_d was influenced by NSS- SO_4^{2-} , NO_3^- , pollution-derived
159 trace elements, and elemental carbon (EC), signifying that species other than SO_4^{2-} influenced
160 N_d . Despite the sampling site's proximity to African deserts, the mass concentration of crustal
161 elements contained in dust was found to have little correlation with N_d . Also, the sea salt tracer
162 sodium (Na^+) was found to have little correlation with N_d . Several studies (e.g., Boucher &
163 Lohmann, 1995; Lowenthal et al., 2004; Menon et al., 2002; Van Dingenen et al., 1995) have
164 combined field data, such as those mentioned above, in addition to other data sets, with the
165 intention of producing a robust empirical prediction of N_d . Menon et al. (2002) provided a log-
166 log multi-species prediction of N_d using SO_4^{2-} , organic matter, and sea salt. Organic carbon has
167 been shown to increase N_d , as it affects the surface tension of cloud droplets (e.g., Facchini et al.,
168 1999; Nenes et al., 2002). Additionally, nitric acid (HNO_3) has been linked with increased CCN
169 activity and N_d based on modeling studies (Hegg, 2000; Kulmala et al., 1993; Xue & Feingold,
170 2004).

171 McCoy et al. (2017) used N_d data from the Moderate-Resolution Imaging
172 Spectroradiometer (MODIS) satellite instead of in situ measurements. Second, aerosol mass
173 concentration data were obtained from the Modern-Era Retrospective Analysis for Research and
174 Applications version 2 (MERRA-2; Gelaro et al., 2017) reanalysis product and various aerosol
175 transport models instead of in situ measurements. Third, the study region was more global in
176 nature (albeit focusing on marine stratocumulus clouds) instead of a specific region. Fourth,
177 since reanalysis data were used, a multi-species, multi-variable linear regression was performed:

$$179 \log(N_d) = a_0 + a_1 \log(\text{SO}_4^{2-}) + a_2 \log(\text{SS}) + a_3 \log(\text{BC}) + a_4 \log(\text{OC}) + a_5 \log(\text{DU}) \quad (2)$$

180
181 where SS is sea salt, BC is black carbon, OC is organic carbon, and DU is dust. McCoy et al.
182 (2017) found that SO_4^{2-} was predominantly correlated with N_d , with sea salt, black carbon,
183 organic carbon, and dust accounting for smaller contributions.



184 The field studies cited above still leave a series of unanswered questions that the current
185 study aims to address: (i) How is the SO_4^{2-} - N_d relationship affected by vertical wind speed
186 (Leaitch et al., 1992), turbulence (Leaitch et al., 1996), and entrainment (Novakov et al., 1994)?;
187 (ii) Why do species such as sea salt and dust play such a minor role in influencing N_d , even when
188 located over the ocean and near a desert (Borys et al., 1998; McCoy et al., 2017, 2018)?; (iii)
189 What is the relationship between organic matter and N_d (McCoy et al., 2018; Nenes et al.,
190 2002)?; and (iv) Can the SO_4^{2-} - N_d correlation be improved by considering other chemical species
191 (e.g., Hegg et al., 1993; Leaitch et al., 1992; Novakov & Penner, 1993)? The present study will
192 examine these questions using a data set comprised of in situ aircraft measurements collected off
193 the California coast during four field campaigns. In addition to meteorological and aerosol and
194 cloud microphysical measurements, a total of 385 cloud water samples were collected and
195 analyzed for 79 chemical species (ions and elements). Even though measurements were collected
196 in only one localized region, it is expected that the variety of conditions encountered over four
197 summers, together with the large number of chemical species analyzed, will help address the
198 questions noted above. The results of this work have implications for simulations and retrievals
199 of N_d , in addition to studies examining relationships between atmospheric chemistry and cloud
200 microphysics.

201

202 **2. Methodology**

203 **2.1. Aircraft campaigns**

204 This work reports results relevant to warm marine stratocumulus clouds off the California
205 coast based on field measurements from four field campaigns between 2011 and 2016, each
206 during the months of July and August. For all field campaigns, the Center for Interdisciplinary
207 Remotely-Piloted Aircraft Studies (CIRPAS) Twin Otter was deployed with an almost identical
208 instrumentation payload. The four campaigns addressed in this study are: the Eastern Pacific
209 Emitted Aerosol Cloud Experiment (E-PEACE) (Russell et al., 2013; Wonaschütz et al., 2013),
210 the Nucleation in California Experiment (NiCE) (Crosbie et al., 2016; Maudlin et al., 2015), the
211 Biological and Oceanic Atmospheric Study (BOAS) (Wang et al., 2016), and the Fog and
212 Stratocumulus Evolution (FASE) Experiment (Dadashazar et al., 2017; MacDonald et al., 2018).
213 Research flight information and tracks are shown in Table 1 and Figure 1, respectively.

214

215 **2.2. Aircraft instrumentation**

216 Aircraft instrumentation used in each campaign is described in detail in Sorooshian et al.
217 (2018). The relevant instrumentation used in the present study is as follows: aerosol size
218 distribution was measured using a Passive Cavity Aerosol Spectrometer Probe (PCASP; particle
219 diameter (D_p) \sim 0.1–2.6 μm ; Strapp et al., 1992); cloud droplet size distribution was measured
220 using a Forward Scattering Spectrometer Probe (FSSP; $D_p \sim$ 2–45 μm ; Gerber et al., 1999) and a
221 Cloud and Aerosol Spectrometer-Forward Scattering (CASF; $D_p \sim$ 1–61 μm ; Baumgardner et al.,
222 2001); rain drop size distribution was measured using a Cloud Imaging Probe (CIP; $D_p \sim$ 25–
223 1600 μm ; Baumgardner et al., 2001); cloud liquid water content (LWC) was measured using a
224 Particulate Volume Monitor (PVM-100A; $D_p \sim$ 3–50 μm ; Gerber, 1994); three-dimensional wind
225 speeds were calculated by combining the pressure measurements from a five-hole radome gust
226 probe plumbed into the aircraft nose together with the aircraft velocity and altitude
227 measurements provided by the aircraft's Global Positioning System/Inertial Navigation System
228 (GPS/INS).



229 Since LWC played a critical role in converting aqueous concentration to air-equivalent
230 concentration, the size range used to calculate N_d was bracketed to resemble the size range of the
231 PVM-100A. Therefore, N_d was defined in this study to be equivalent to the integration of the
232 cloud droplet size distribution between $D_p \sim 3\text{--}50 \mu\text{m}$, and was calculated using CASF (for E-
233 PEACE) and FSSP (NiCE, BOAS, and FASE). For the NiCE campaign, LWC measurements
234 from the PVM-100A instrument were unreliable; therefore, the LWC for NiCE was calculated
235 instead using FSSP data between $D_p \sim 3\text{--}50 \mu\text{m}$.

236

237 **2.3. Cloud water collection and chemical analysis**

238

239 A total of 385 cloud water samples were collected throughout the four campaigns using a
240 modified Mohnen slotted-rod collector, reported to collect droplets with $D_p \sim 5\text{--}35 \mu\text{m}$ (Hegg and
241 Hobbs, 1986). The cloud water was collected in polyethylene bottles and stored at $\sim 5^\circ\text{C}$ for
242 subsequent offline chemical analysis. The spatially-averaged location of each cloud water sample
243 is shown in Figure 1. Cloud water samples were chemically analyzed post-flight for ions using
244 ion chromatography (IC; Dionex ICS-2100) and for elements using inductively coupled plasma
245 mass spectrometry (ICP-MS; Agilent 7700 Series) for E-PEACE, BOAS, and NiCE or triple
246 quadrupole inductively coupled plasma mass spectrometry (ICP-QQQ; Agilent 8800 Series) for
247 FASE. The limit of detection (LOD) for each ion and element measured is shown in Table S1.
248 The concentration of non-sea salt (NSS) species was calculated using the relative abundance of a
249 NSS species to Na^+ in natural sea salt (Seinfeld & Pandis, 2016). Aqueous concentrations (i.e.,
250 mass concentrations in the droplets [mg L^{-1}]) were converted to air-equivalent concentrations
251 (i.e., mass concentrations in the air [$\mu\text{g m}_{\text{air}}^{-3}$]) by multiplying aqueous concentrations by the
252 LWC and dividing by the mass density of water.

253

254 A total of 79 species (29 measured ionic species, 46 measured elemental species, and 4
255 NSS calculated species; Table 2) were considered in this study as an initial pool of candidate
256 species that could potentially be used to predict N_d . To facilitate the statistical analysis in this
257 study, the amount of chemical species were filtered from 79 to only nine. The steps used in this
258 filtering process are summarized in the next section.

259

260 **2.4. Filtering of chemical species**

261

262 A focus in this study is to identify appropriate chemical species to use as predictors in a
263 linear regression model (addressed in Section 2.5). Good statistical practice (e.g., Freund et al.,
264 2010) recommends that two conditions must be met to produce a meaningful multivariable
265 regression: (1) the independent/predictor variables must not be redundant, i.e., they must not be
266 highly correlated among themselves (the property of high correlation is called collinearity), and
267 (2) each independent/predictor variable must have some correlation with the dependent/response
268 variable. There is no universal rule to define what is “highly” correlated, rather, it depends on the
269 nature of the data and the user’s judgement.

270

271 As using all 79 species is impractical in terms of providing results that could be tested
272 and/or used by others, a filtering method was used to reduce the number of species. The filtering
273 method consisted of seven steps (Figure 2), the objective of which was to trim the total number
274 of species by an order of magnitude, leaving just a few that exhibited the following
275 characteristics: (1) the most data quality and quantity, (2) the least redundancy among
276 themselves, (3) the highest correlation with N_d , and (4) the most physical meaning. The decision
277 to remove a species becomes less objective and quantifiable towards the last steps in Figure 2.
278 Each step is described below.



275 Step 1 removed species with less than 70% of data points. A species could have a low
276 amount of points because it was not analyzed in a field campaign or because the data quality
277 from the IC or ICP (ICP-MS or ICP-QQQ) was inadequate. Step 2 removed duplicate species
278 that were measured by both IC and ICP. Step 3 addressed Condition (2) by removing species that
279 were collinear (i.e., correlated among themselves). The criterion for a “high” correlation was to
280 have a correlation coefficient (R) > 0.6 and a p-value < 0.05 . For example, if a fixed number of
281 five species were all highly correlated between each other, then only one of the five species was
282 kept, and the rest were removed. This procedure is to consolidate “families” of three or more
283 highly correlated species to a single species and does not apply to pairs of highly consolidated
284 species. Step 4 addressed Condition (3) by removing species that were not correlated to N_d . The
285 criterion for a “low” correlation was to have a coefficient of determination (R^2) < 0.1 . Notice that
286 Step 3 uses R whereas Step 4 uses R^2 ; this is because collinearity is determined not only by the
287 value of R but also the sign of R . Step 5 removes all but one organic species, oxalate (Ox), since
288 this species generally had the highest mass concentration of all the organic species and was
289 considered to be representative of all other organic species. Step 6 removed species that could
290 not easily be attributed to a physical process or chemical source. Step 7 added back into the
291 analysis four species that had been removed. This was done for the sake of having species that
292 are known to have relevant sources in the study region.

293 The nine species that survived the filtering scheme in Figure 2 are methanesulfonic acid
294 (MSA), ammonium (NH_4^+), NO_3^- , Ox, Tot- SO_4^{2-} , NSS- SO_4^{2-} , Fe, Na, and vanadium (V). These
295 species have known sources as follows. MSA: ocean biogenic (Sorooshian et al., 2009); NH_4^+ :
296 agriculture (Bauer et al., 2016), marine emissions (Bouwman et al., 1997), and wildfires (Reid
297 et al., 1998); NO_3^- : and Ox: fire (Prabhakar et al., 2014; Maudlin et al., 2015); Tot- SO_4^{2-} : sea salt
298 (Seinfeld & Pandis, 2016), ocean biogenic (Charlson et al., 1987), and shipping (Coggon et al.,
299 2012), with NSS- SO_4^{2-} missing the sea salt contribution; Fe: dust (Jickells et al., 2005) and fire
300 (Maudlin et al., 2015); Na: sea salt (Seinfeld & Pandis, 2016); V: shipping (Wang et al., 2014).
301 Note that we retained both Tot- SO_4^{2-} and NSS- SO_4^{2-} ; this is to evaluate which correlates more
302 with N_d , as some studies have used Tot- SO_4^{2-} (e.g., Leaitch et al., 1992; Saxena & Menon, 1999),
303 whereas other have used NSS- SO_4^{2-} (Novakov et al., 1994; Boucher & Lohmann, 1995).
304 Sections 3.1 and 3.2 will discuss these nine species, and the rest of Section 3 will focus on only
305 four species to be explained later. These species were analyzed by a multivariable regression
306 model, which is described in the next section.

307

308 2.5. Mathematical model

309 This study examines the relationship between cloud water mass concentration and N_d
310 with a multivariable linear model similar to that of McCoy et al. (2017, 2018):

311

$$312 \log(N_d) = a_0 + a_1 \log(M_1) + a_2 \log(M_2) + \dots + a_n \log(M_n) \quad (3)$$

313

314 where M_i is the air-equivalent mass concentration of species i [$\mu\text{g m}^{-3}$], a_i are fitting parameters,
315 and n is the number of species being considered. N_d is the dependent (or response) variable, and
316 M_1, M_2, \dots, M_n are the independent (or predictor) variables. The logarithmic forms of N_d and M_i
317 were correlated to account for a numerically large range of several orders of magnitude, and
318 because a log-log model is commonly used to correlate chemical composition to N_d (e.g.,
319 Boucher & Lohmann, 1995; Menon et al., 2002; McCoy et al., 2017).



320 The Matlab software package was used to obtain multivariable linear regressions of the
321 form of Equation 3 using the method of ordinary least squares. The performance of a regression
322 was quantified using the coefficient of determination (R^2). However, when comparing the
323 performance of correlations between regressions using a different number of predictor variables,
324 it is necessary to use the adjusted coefficient of determination (R_{adj}^2), which is subscripted to
325 distinguish it from the ordinary R^2 (Kahane, 2008). For the sake of consistency, R_{adj}^2 is used
326 instead of the ordinary R^2 , except when reporting values from the literature. The statistical
327 significance of correlations was quantified using the p-value obtained by doing a two-tailed
328 Student's t-test. Both R_{adj}^2 and p-values were given by the Matlab software after regression. P-
329 values were obtained for both the overall regression and each individual coefficient in the
330 regression, e.g., if a regression has three predictors, there are a total of five p-values: one for the
331 overall regression, three for the slope of each individual predicting variable, and one for the
332 intercept. In this study, a regression was considered to be statistically significant if all the p-
333 values were < 0.05 .

334

335 **2.6. Calculation of turbulence**

336

337 Similar to Leaitch et al. (1992) and Feingold et al. (1999), this study analyzes the effect
338 of turbulence on the ability to predict N_d . Turbulence was considered to be represented by the
339 standard deviation of the vertical wind speed (w) and is represented as σ_w . Also similar to Leaitch
340 et al. (1992), this study classified conditions into turbulent and smooth regimes by considering
341 the upper and lower 33 percentile of σ_w , respectively. Although the rigorous approach to
342 calculate σ_w uses the w from below the cloud (Twomey, 1959), this study used vertical wind
343 speed data collected throughout the sampling time (i.e., mostly inside the cloud, but also outside
344 the cloud). This was mainly because not all cloud water samples had an accompanying
345 measurement of w below the cloud. To justify using σ_w from the sampling time instead of below
346 cloud σ_w , consider Figure S1, which shows a representative time series of altitude, w , and σ_w for
347 a cloud water sample that was collected minutes before a below-cloud leg, which collected
348 measurements of w . It can be seen that the plots of w and σ_w are similar, and that an average σ_w
349 calculated either way is still in the bottom 33rd percentile. Therefore, for purposes of this study,
350 we consider in-cloud turbulence to reasonably approximate below-cloud turbulence.

350

351 **2.7. Determination of smoke influence**

352

353 One of the objectives of this study is to analyze the extent to which the presence of
354 smoke from wildfires affects the correlation between N_d and cloud water chemical composition.
355 Thus, it was important to identify cloud water samples that were influenced by smoke. Only the
356 NiCE and FASE campaigns were affected by wildfires. Mardi et al. (2018) identified vertical
357 soundings in the NiCE and FASE campaigns that were influenced by smoke by establishing
358 smoke influence to have a total aerosol number concentration (N_d) $\geq 1000 \text{ cm}^{-3}$, as measured by
359 the PCASP, in addition to visual and olfactory detection of smoke by flight scientists. In this
360 study, a cloud water sample was considered to be influenced by smoke if it was collected during
361 a research flight (RF) that contains a vertical sounding identified by Mardi et al. (2018) to be
362 influenced by smoke, even if the cloud water sample was not necessarily collected near the
363 sounding labelled as smoke-influenced; this is a valid assumption based on the work of Mardi et
364 al. (2019). The RFs considered to be smoke-influenced in this study were NiCE RFs 16—23 and
365 FASE RFs 3—11 and 13—15.

365



366 3. Results and Discussion

367 With the refined list of nine physically-meaningful species from Section 2.4, we now
368 proceed to address the following questions: (1) What single species best predicts N_d ?; (2) How
369 many species are sufficient to predict N_d ?; (3) What is an effective combination of species to
370 predict N_d ?; and (4) How do several factors (i.e., turbulence, smoke-influence, and location along
371 cloud depth) affect the ability to reliably predict N_d ? These questions are addressed in order in
372 Sections 3.1–3.4.
373

374 3.1. Single-variable prediction of N_d

375 In this section, we analyze which of the nine species filtered out in Section 2.4 best
376 predicts N_d by itself without binning by external factors. These single-predictor regressions with
377 no binning are important, as they provide a baseline for subsequent sections in which multi-
378 predictor regressions and binning are used. Table 3 and Figure 3 display the ability of each of the
379 nine species to predict N_d . To have consistency with subsequent sections, R^2_{adj} is used instead of
380 the ordinary R^2 . The regression and the individual coefficients all were statistically significant.

381 Some previous studies predicted N_d using Tot-SO₄²⁻ (e.g., Leaitch et al., 1992; Saxena &
382 Menon, 1999), whereas other studies used NSS-SO₄²⁻ (e.g., Novakov et al. 1994; Lowenthal et
383 al., 2004). We find that Tot-SO₄²⁻ is the best predictor, and that is better correlated to N_d ($R^2_{adj} =$
384 0.40) than NSS-SO₄²⁻ ($R^2_{adj} = 0.29$). This is likely because Tot-SO₄²⁻ encompasses both sea salt
385 particles and non-sea salt particles, and thus gives a better approximation to the total number
386 concentration of CCN. In addition, Tot-SO₄²⁻ also had the largest slope ($a_1 = 0.32$), suggesting
387 that N_d is more sensitive to changes in Tot-SO₄²⁻ than other chemical species. Although HNO₃
388 has been observed to increase N_d (e.g., Xue & Feingold, 2004), NO₃⁻ was found to be only
389 moderately correlated with N_d ($R^2_{adj} = 0.24$). The species with the lowest correlation was Fe
390 ($R^2_{adj} = 0.05$). This low correlation with N_d was also presented by other crustal metals that like Al
391 ($R^2_{adj} = 0.01$) and Ti ($R^2_{adj} \sim 0$) (not shown in Table 3). The low influence of crustal metals on N_d
392 is consistent with the findings of Lowenthal & Borys (2000). Some physical meaning can be
393 extracted from the intercept of the regression (a_0). If N_d is insensitive to the mass concentration
394 of a species, then the slope (a_1) should be zero; and N_d would be constant with a value of $N_d =$
395 10^{a_0} . These intercepts yield a range of N_d of 108–412 cm⁻³. These values are not unrealistic in
396 clouds in this study region (e.g., Chen et al., 2012; Lu et al., 2009; Wang et al., 2016).
397

398 To contrast with results of this work, Table 4 shows the regression parameters from other
399 studies when correlating N_d and SO₄²⁻. For the sake of completeness, Table 4 shows regressions
400 that analyzed non-marine stratocumulus clouds, but in this comparison, we focus only on those
401 regressions that analyzed stratocumulus clouds. Our results (i.e., a_i coefficients and R^2) for Tot-
402 SO₄²⁻ reasonably match the results of Leaitch et al. (1992), suggestive of commonality between
403 two ocean regions with differing meteorological conditions (i.e., northeast Pacific vs northwest
404 Atlantic) (Sorooshian et al., 2019). Our results for NSS-SO₄²⁻ also reasonably match those of
405 McCoy et al. (2017), which is noteworthy as McCoy et al. (2017) used satellite retrievals and
406 model aerosol concentrations for several stratocumulus decks around the world, whereas our
407 analysis used in situ data from a relatively small region. However, our NSS-SO₄²⁻ results differ
408 significantly from those of Novakov et al. (1994), which is understandable since the regression
409 presented by Novakov et al. (1994) has a p-value > 0.05. Our data set does not achieve the
410 degree of correlation achieved by Lowenthal et al. (2004), who report the highest correlation for
411 marine clouds ($R^2 = 0.82$). The studies that analyzed stratocumulus clouds all report intercept
values (a_0) ~ 2.0 , which is consistent with our data.



412

413 3.2. Multi-variable prediction of N_d

414 When previous studies correlated N_d (or N_{CCN}) and the air-equivalent concentration of
415 chemical species and obtained a poor correlation, it was suggested that taking more chemical
416 species into consideration would improve the correlation (e.g., Leaitch et al., 1992; Novakov et
417 al., 1994). In this section we address the issue: “How many chemical species are necessary
418 to adequately predict N_d ?”. To answer this question, we use the nine filtered species from Section
419 2.4. Regressions of the form of Equation 3 are performed for every combination of species. The
420 number of predictors in the regressions are varied from one up to eight. The number of
421 combinations (C) that can be made with P predictors selected from S species is $C = S!/(S - P)!$.
422 Combinations that include Tot-SO₄²⁻ and NSS-SO₄²⁻ together are not considered, thus leaving a
423 total of 383 regressions.

424 Of the total 383 regression, only 67 were considered as statistically significant. Figure 4
425 shows the R^2_{adj} as a function of the number of predictors for both statistically significant and
426 insignificant regressions; the percentage of regressions that were statistically significant is shown
427 in Table S2. These results show that adding more predictors does not necessarily improve the
428 correlation, as all correlations that use six or more predictors are statistically insignificant. This
429 behavior is perhaps because the new species being added are redundant with respect to the
430 species that are already in the model (i.e., the new species is mathematically collinear with the
431 old species). It is also interesting to note how R^2_{adj} increases asymptotically to ~ 0.6 ; this further
432 makes the point that additional species do not necessarily improve predictability of N_d .

433 We examined the best regressions produced by a given number of predictors to explore
434 the factors that contribute to a respectable multivariable regression. Table 5 shows the three
435 statistically significant regressions that had the highest R^2_{adj} for a given number of predictors
436 (one to five). The predictors are ordered horizontally according to the value of their coefficient in
437 order to show qualitatively which species is more dominant in a regression. Eight of the nine
438 chemical species considered appear at least once in a regression, with the most common species
439 being NH₄⁺, a form of SO₄²⁻ (total or non-sea salt), Na, Ox, and MSA. Sulfate (total or non-sea
440 salt) appears in 12 of the 15 regressions, and in eight regressions it has the largest coefficient;
441 this speaks to the importance of SO₄²⁻ in predicting N_d . However, the appearance of Na and Ox
442 and their non-negligible slope also highlights the importance of considering them as well in a
443 correlation; this is clearly observed in the increase of R^2_{adj} when Na and Ox are added to a
444 regression that contains only NSS-SO₄²⁻ (Table 6). We believe that the ingredients that yield the
445 higher R^2_{adj} in Table 6 are: (1) a form of SO₄²⁻ (such Tot-SO₄²⁻ or NSS-SO₄²⁻), (2) a sea
446 emissions tracer (such as Na), and (3) an organic tracer (such as Ox). NH₄⁺ was present in all the
447 regressions; however, given that it comes from diverse sources such as agriculture (ApSimon et
448 al., 1987; Bauer et al., 2016), marine emissions (Bouwman et al., 1997; Paulot et al., 2015), and
449 wildfires (Maudlin et al., 2015; Reid et al., 1998), it is difficult to assess if it contributes to the
450 CCN budget or simply accompanies all types of CCN. In other words, we suspect that NH₄⁺
451 appears in all correlations because it generally accompanies the three ingredients we propose
452 make a good correlation: a form of SO₄²⁻, a marine emissions tracer, and an organic tracer.

453 It is of interest to note that combining a sea salt tracer (such as Na) with NSS-SO₄²⁻ in a
454 two-predictor model has about the same performance ($R^2_{adj} = 0.41$; Table 6) as a one-predictor
455 model using Tot-SO₄²⁻ ($R^2_{adj} = 0.40$; Table 3). We believe this is because Tot-SO₄²⁻ encompasses
456 the sea salt and the non-sea salt contribution to CCN about the same as the artificial
457 mathematical separation of the two. Also of interest is that when only looking at the statistically



458 significant regressions, only 17 regressions have species with negative coefficients (i.e., negative
459 slopes). The species with negative coefficients are NO_3^- , Fe, and V (not shown); more
460 specifically, NO_3^- , Fe, and V have negative coefficients when they are accompanied by NH_4^+ in
461 the same regression. The physical reason as to why these species have negative coefficients
462 when mixed with NH_4^+ is not clear; perhaps the reason is due to the mathematics of the
463 regression and not physically rooted, as multicollinearity can lead to unexpected signs for
464 predictor coefficients (Kahane, 2008).

465 Menon et al. (2002) and McCoy et al. (2017, 2018) are among the few studies that have
466 used multiple species to predict N_d (Table 7). Menon et al. (2002) used three species (sulfate,
467 organic matter, and sea salt). McCoy et al. (2017, 2018) used five species (sulfate, sea salt, black
468 carbon, organic carbon, and dust), but the 2017 study found the contribution of organic matter to
469 be negligible. McCoy et al. (2017) observed a negative coefficient for sea salt (i.e., more sea salt
470 leads to fewer cloud droplets); however, we do not observe the same trend in our results, as the
471 sea salt tracer (Na) always has a positive coefficient. In order to intercompare results with
472 previous studies, we selected species homologous to those of McCoy et al. (2017, 2018). We
473 select NSS-SO_4^{2-} for sulfate, Na for sea salt, oxalate for organic carbon, and Fe for dust. We did
474 not measure a species analogous to black carbon. The subsequent analysis examines only these
475 four species using single-predictor regressions.

476

477 3.3. Analysis of meteorological factors through binning

478 Historically, the effect that meteorological factors have on the composition- N_d (or $-N_{CCN}$)
479 empirical relationship has been examined by analyzing regressions after binning by turbulence
480 (Leaitch et al., 1996), cloud type (Leaitch et al., 1992; Novakov & Penner, 1993), and region
481 (McCoy et al., 2018). The following sections address the effects of turbulence, smoke influence,
482 and location along cloud depth.

483

484 3.3.1. Effect of turbulence

485 Building upon the work of Leaitch et al. (1996), who studied how turbulence affects the
486 correlation between Tot-SO_4^{2-} and N_d , this study extends that analysis to examine four additional
487 species. Similar to Leaitch et al. (1996), this study quantified turbulence by the standard
488 deviation of vertical wind speed (σ_w). Our range of σ_w was 0.10–0.51 m s^{-1} . Low turbulence was
489 considered to be in the bottom 33rd percentile ($\leq 0.27 \text{ m s}^{-1}$), whereas high turbulence was taken
490 to be values in the top 33rd percentile ($\geq 0.33 \text{ m s}^{-1}$). Leaitch et al. (1996) considered low and high
491 turbulence to be $\sigma_w < 0.17 \text{ m s}^{-1}$ and $\sigma_w > 0.23 \text{ m s}^{-1}$, respectively, and it is worth noting that only
492 five of our 385 samples are considered low turbulence according to the criterion of Leaitch et al.
493 (1996). Figure 5 and Table 8 show how R^2_{adj} depends on the predicting species and the
494 turbulence regime; the scatterplots from which the R^2_{adj} are taken are shown in Figure S2.

495 For NSS-SO_4^{2-} , there is no significant difference in R^2_{adj} when comparing all the points or
496 by binning by σ_w . However, this is not the case for Tot-SO_4^{2-} , in which there is a large difference
497 in the degree of correlation ($R^2_{adj} = 0.27$ and $R^2_{adj} = 0.55$ for low σ_w and high σ_w , respectively).
498 This is in agreement with Leaitch et al. (1996), in which the correlation (albeit, not log-log)
499 between Tot-SO_4^{2-} and N_d yielded an $R^2 = 0.53$ and $R^2 = 0.91$ for low and high σ_w , respectively.
500 The difference in the behavior between Tot-SO_4^{2-} and NSS-SO_4^{2-} hints that the sea salt
501 contributions to SO_4^{2-} (i.e., ocean-derived species) are the ones affected by turbulence, and hence
502 explains the insensitivity NSS-SO_4^{2-} has to turbulence.



503 For Na, there is a better correlation at high turbulent conditions than at smooth conditions
504 ($R^2_{adj} = 0.26$ and $R^2_{adj} = 0.09$ for high and low σ_w , respectively). This further strengthens the
505 argument that turbulence plays an important role in the vertical transport of sea salt (and other
506 ocean emissions) from the ocean surface to the cloud base.

507 For Ox, the correlation improves at low turbulence ($R^2_{adj} = 0.30$), but not at high
508 turbulence ($R^2_{adj} = 0.09$). We believe Ox behaves differently than Na because it does not
509 necessarily just enter the cloud from below via updrafts, but rather it enters the cloud from above
510 via entrainment of air from the free troposphere that can at times be enriched with organic
511 species in the study region (Coggon et al., 2014; Crosbie et al., 2016; Hersey et al., 2009;
512 Sorooshian et al., 2007).

513 For Fe, all turbulence scenarios yield a low correlation between Fe and N_d , indicating
514 that, overall, Fe is not a good predictor for N_d .

515

516 3.3.2. Effect of smoke influence

517 The clouds in the study region are affected by the smoke from wildfires (e.g., Dadashazar
518 et al., 2019; Maudlin et al., 2015; Schlosser et al., 2017). As mentioned in Section 2.7, Mardi
519 et al. (2018) used the same data set as this study and identified research flights (RFs) that contained
520 smoke-influenced cloud soundings, namely NiCE RFs 16—23 and FASE RFs 3—11 and 13—
521 15. In this study, we considered that all cloud water samples collected during the aforementioned
522 RFs were influenced by smoke. Furthermore, we did not distinguish if the smoke was above or
523 below in the cloud; this is an important caveat, as cloud microphysical properties seem to depend
524 on the surrounding smoke vertical profile (e.g., Diamond et al., 2018; Koch & Del Genio, 2010).
525 The correlation between N_d and composition as a function of smoke influence is shown in Figure
526 6 and Table 8, and the scatterplots from which the R^2_{adj} are taken are shown in Figure S3.
527 Species that are produced during wildfires exhibited an improvement in R^2_{adj} when considering
528 only the smoke-influenced cases. The opposite is true for species not produced during wildfires.
529 More specifically, Ox and Fe showed an increase in correlation for smoke-influenced conditions
530 ($R^2_{adj} = 0.42$ and $R^2_{adj} = 0.15$ for Ox and Fe, respectively) and a small decrease in for smoke-free
531 conditions ($R^2_{adj} = 0.07$ and $R^2_{adj} = 0.04$ for Ox and Fe, respectively). This is most likely because
532 Ox and Fe concentrations increase during wildfires (e.g., Maudlin et al., 2015) and thus
533 contribute appreciably to the regional CCN during the summertime when wildfires are prevalent.

534 NSS-SO₄²⁻ and Na showed a decrease in correlation for smoke-influenced conditions
535 ($R^2_{adj} = 0.22$ and $R^2_{adj} = 0.17$ for NSS-SO₄²⁻ and Na, respectively), and an increase for smoke-
536 free conditions ($R^2_{adj} = 0.36$ and $R^2_{adj} = 0.24$ for NSS-SO₄²⁻ and Na, respectively). We suspect
537 this is because even though wildfires can produce NSS-SO₄²⁻ (e.g., Reid et al., 1998) and Na
538 (e.g., Hudson et al., 2004; Silva et al., 1999), these species are not produced as effectively as Ox
539 or Fe. For example, Maudlin et al. (2015) measured aerosol mass concentration in the study
540 region during both smoke-influenced and non-smoke-influenced conditions. They reported an
541 increase in mass concentration for NSS-SO₄²⁻, Na, Ox, and Fe to be 30%, 120%, 220%, and
542 408%, respectively, for submicron particles, and -2%, -28%, 164%, and 97%, respectively, for
543 supermicrometer particles. Consequently, Ox and Fe are produced more in wildfires in the study
544 region than NSS-SO₄²⁻ and Na.

545

546 3.3.3. Effect of in-cloud height

547 MacDonald et al. (2018) used the same data set as this study to show that the chemical
548 composition of cloud water varies with height within a cloud. It is therefore reasonable that the



549 N_d -chemical composition relationship also varies with in-cloud height. The correlation between
550 N_d and composition as a dependence of in-cloud height is shown in Figure 7 and Table 8, and the
551 scatterplots from which the R^2_{adj} are taken are shown in Figure S4.

552 Ox and Fe exhibit a better correlation when focusing on the bottom third of the cloud
553 ($R^2_{adj} = 0.29$ and $R^2_{adj} = 0.20$ for Ox and Fe, respectively). When focusing on the top third of the
554 cloud, the correlation decreased for Ox ($R^2_{adj} = 0.08$) and remained unchanged for Fe ($R^2_{adj} =$
555 0.03). One possible hypothesis to explain why Ox and Fe are better predictors of N_d at cloud base
556 is that smoke affects cloud microphysics (N_d and effective radius) more at cloud base than at
557 cloud top, regardless of whether the smoke was above or below the cloud (Diamond et al., 2018;
558 Mardi et al., 2019).

559 NSS-SO₄²⁻ and Na exhibit a better correlation with N_d when focusing on the top third of
560 the cloud ($R^2_{adj} = 0.33$ and $R^2_{adj} = 0.33$ for NSS-SO₄²⁻ and Na, respectively). The correlation
561 decreases when focusing on the bottom third of the cloud ($R^2_{adj} = 0.17$ and $R^2_{adj} = 0.10$ for NSS-
562 SO₄²⁻ and Na, respectively). Tot-SO₄²⁻ also follows this pattern ($R^2_{adj} = 0.56$ and $R^2_{adj} = 0.22$ for
563 top and bottom, respectively).

564 It is not entirely clear why NSS-SO₄²⁻ and Na would be better correlated with N_d in the
565 top third of clouds. MacDonald et al. (2018) noted that the concentration of chemical species
566 varies as a function of in-cloud height and is not the same for all species; the concentration of Na
567 is greatest at cloud base whereas that of NSS-SO₄²⁻ and Ox are greatest mid-cloud. It would be
568 expected that the vertical profile of concentration is related to the ability to predict N_d (i.e., that a
569 larger concentration of a species leads to a better correlation with N_d), but that expectation is not
570 observed in these results. It is also interesting to point out that there is not much difference in
571 R^2_{adj} when considering all cloud thirds versus only the middle third; this makes sense, as almost
572 half of the cloud water samples (46%) were collected in the middle third of the cloud.

573 The dependence of the correlation between chemical composition and N_d on in-cloud
574 height is of relevance to remote sensing, which relies on satellite measurement of cloud top
575 properties such as cloud top temperature to then calculate a constant N_d throughout the cloud
576 depth (e.g., Grosvenor et al., 2018).

577

578 4. Conclusions

579 This study used a four-year data set of airborne measurements collected in warm marine
580 stratocumulus clouds off the California coast and analyzed the extent to which the chemical
581 composition of cloud water can be used to predict N_d . A total of 79 species were filtered to nine
582 to examine the prediction of N_d using a single-species model, and then using a multi-species
583 model. The 79 species were subsequently filtered to four to examine how the four single-species
584 models were affected by environmental factors, namely, turbulence, smoke influence, and
585 vertical location within a cloud. The most important findings of this paper are:

586

- 587 1. The species that best predicted N_d is Tot-SO₄²⁻ with $R^2_{adj} = 0.40$, followed by NH₄⁺ ($R^2_{adj} =$
588 0.34), NSS-SO₄²⁻ ($R^2_{adj} = 0.29$), MSA ($R^2_{adj} = 0.26$), and NO₃⁻ ($R^2_{adj} = 0.24$).
- 589 2. The prediction of N_d can be improved by using a multi-species model. However, increasing
590 the number of species caused the R^2_{adj} to asymptotically approach ~ 0.6 . Furthermore, the
591 regressions with six or more species became statistically insignificant.
- 592 3. Analyzing the three best correlations for each of the n -species models (where $n = 1-5$)
593 shows that the factors that constitute a good regression are: a form of SO₄²⁻ (total or non-sea
594 salt), an ocean emissions tracer, and an organic tracer.



- 595 4. Greater turbulence (approximated as the standard deviation of vertical wind speed) improves
596 the ability of ocean-derived species to predict N_d , as observed when comparing regressions
597 using turbulent data points versus all data points for Tot-SO₄²⁻ ($\Delta R^2_{adj} = 0.15$) and Na (ΔR^2_{adj}
598 = 0.07), but not for NSS-SO₄²⁻ ($\Delta R^2_{adj} = -0.01$) or Ox ($\Delta R^2_{adj} = -0.06$).
- 599 5. The influence of smoke significantly affects those species that best predict N_d . Ox (a species
600 known to be produced during biomass burning) was best correlated with N_d ($R^2_{adj} = 0.42$)
601 under smoke-influenced conditions.
- 602 6. Vertical location within the cloud affects the ability to predict N_d . The species that are best
603 correlated with N_d at cloud top are Tot-SO₄²⁻ ($R^2_{adj} = 0.56$) and NSS-SO₄²⁻ ($R^2_{adj} = 0.33$);
604 those best correlated with N_d at cloud base are fire tracers such as Ox ($R^2_{adj} = 0.29$) and Fe
605 ($R^2_{adj} = 0.20$), as it has been reported that the base of a cloud is more sensitive to the
606 influence of smoke.



607 **Data Availability**

608 All data used in this work can be found on the Figshare database (Sorooshian et al., 2018;
609 [https://figshare.com/articles/A_Multi-Year_Data_Set_on_Aerosol-Cloud-Precipitation-
610 Meteorology_Interactions_for_Marine_Stratocumulus_Clouds/5099983](https://figshare.com/articles/A_Multi-Year_Data_Set_on_Aerosol-Cloud-Precipitation-Meteorology_Interactions_for_Marine_Stratocumulus_Clouds/5099983)).

611

612 **Author Contributions**

613 All coauthors contributed to some aspect of the data collection. ABM and AS conducted
614 the data analysis and interpretation. ABM and AS prepared the manuscript with contributions
615 from all coauthors.

616

617 **Competing Interests**

618 The authors declare that they have no conflict of interest.

619

620 **Acknowledgements**

621 Alexander B. MacDonald acknowledges support from the Mexican National Council for
622 Science and Technology (CONACYT). We acknowledge Agilent Technologies for their support
623 and Shane Snyder's laboratories for ICP-QQQ data.

624

625 **Financial Support**

626 These field campaigns were funded by Office of Naval Research grants N00014-10-1-
627 0811, N00014-11-1-0783, N00014-10-1-0200, N00014-04-1-0118, and N00014-16-1-2567. This
628 work was also partially supported by NASA grant 80NSSC19K0442 in support of the
629 ACTIVATE Earth Venture Suborbital-3 (EVS-3) investigation, which is funded by NASA's
630 Earth Science Division and managed through the Earth System Science Pathfinder Program
631 Office.

632

633



634 **References**

- 635 Abdul-Razzak, H. and Ghan, S. J.: A parameterization of aerosol activation 2. Multiple aerosol
636 types, *J. Geophys. Res.*, 105(D5), 6837–6844, <https://doi.org/10.1029/1999JD901161>,
637 2000.
- 638 Adams, P. J. and Seinfeld, J. H.: Disproportionate impact of particulate emissions on global
639 cloud condensation nuclei concentrations, *Geophys. Res. Lett.*, 30(5), 1239,
640 <https://doi.org/10.1029/2002gl016303>, 2003.
- 641 Albrecht, B. A.: Aerosols, Cloud Microphysics, and Fractional Cloudiness, *Science*, 245(4923),
642 1227–1230, <https://doi.org/10.1126/science.245.4923.1227>, 1989.
- 643 Andreae, M. O. and Rosenfeld, D.: Aerosol-cloud-precipitation interactions. Part 1. The nature
644 and sources of cloud-active aerosols, *Earth-Science Rev.*, 89(1–2), 13–41,
645 <https://doi.org/10.1016/j.earscirev.2008.03.001>, 2008.
- 646 ApSimon, H. M., Kruse, M. and Bell, J. N. B.: Ammonia emissions and their role in acid
647 deposition, *Atmos. Environ.*, 21(9), 1939–1946, [https://doi.org/10.1016/0004-
648 6981\(87\)90154-5](https://doi.org/10.1016/0004-6981(87)90154-5), 1987.
- 649 Bauer, S. E., Tsigaridis, K. and Miller, R.: Significant atmospheric aerosol pollution caused by
650 world food cultivation, *Geophys. Res. Lett.*, 43(10), 5394–5400,
651 <https://doi.org/10.1002/2016GL068354>, 2016.
- 652 Baumgardner, D., Jonsson, H., Dawson, W., O'Connor, D. and Newton, R.: The cloud, aerosol
653 and precipitation spectrometer: A new instrument for cloud investigations, *Atmos. Res.*,
654 59–60, 251–264, [https://doi.org/10.1016/S0169-8095\(01\)00119-3](https://doi.org/10.1016/S0169-8095(01)00119-3), 2001.
- 655 Behrenfeld, M. J., Moore, R. H., Hostetler, C. A., Graff, J., Gaube, P., Russell, L. M., Chen, G.,
656 Doney, S. C., Giovannoni, S., Liu, H., Proctor, C., Bolaños, L. M., Baetge, N., Davie-
657 Martin, C., Westberry, T. K., Bates, T. S., Bell, T. G., Bidle, K. D., Boss, E. S., Brooks, S.
658 D., Cairns, B., Carlson, C., Halsey, K., Harvey, E. L., Hu, C., Karp-Boss, L., Kleb, M.,
659 Menden-Deuer, S., Morison, F., Quinn, P. K., Scarino, A. J., Anderson, B., Chowdhary,
660 J., Crosbie, E., Ferrare, R., Hair, J. W., Hu, Y., Janz, S., Redemann, J., Saltzman, E.,
661 Shook, M., Siegel, D. A., Wisthaler, A., Martin, M. Y. and Ziemba, L.: The North Atlantic
662 Aerosol and Marine Ecosystem Study (NAAMES): Science motive and mission overview,
663 *Front. Mar. Sci.*, 6, 1–25, <https://doi.org/10.3389/fmars.2019.00122>, 2019.
- 664 Borys, R. D., Lowenthal, D. H., Wetzal, M. A., Herrera, F., Gonzalez, A. and Harris, J.:
665 Chemical and microphysical properties of marine stratiform cloud in the North Atlantic, *J.*
666 *Geophys. Res. Atmos.*, 103(D17), 22073–22085, <https://doi.org/10.1029/98JD02087>,
667 1998.
- 668 Boucher, O. and Lohmann, U.: The sulfate-CCN-cloud albedo effect, *Tellus B Chem. Phys.*
669 *Meteorol.*, 47(3), 281–300, <https://doi.org/10.3402/tellusb.v47i3.16048>, 1995.
- 670 Bouwman, A. F., Lee, D. S., Asman, W. A. H., Dentener, F. J., Van Der Hoek, K. W. and
671 Olivier, J. G. J.: A global high-resolution emission inventory for ammonia, *Global*
672 *Biogeochem. Cycles*, 11(4), 561–587, <https://doi.org/10.1029/97GB02266>, 1997.
- 673 Charlson, R. J., Lovelock, J. E., Andreae, M. O. and Warren, S. G.: Oceanic phytoplankton,
674 atmospheric sulphur, cloud albedo and climate, *Nature*, 326(6114), 655–661,
675 <https://doi.org/10.1038/326655a0>, 1987.
- 676 Charlson, R. J., Schwartz, S. E., Hales, J. M., Cess, R. D., Coakley, J. J., Hansen, J. E. and
677 Hofmann, D. J.: Climate forcing by anthropogenic aerosols, *Science*, 117(5043), 423–430,
678 <https://doi.org/10.1126/science.255.5043.423>, 1992.



- 679 Chen, Y. and Penner, J. E.: Uncertainty analysis for estimates of the first indirect aerosol effect,
680 *Atmos. Chem. Phys.*, 5(11), 2935–2948, <https://doi.org/10.5194/acp-5-2935-2005>, 2005.
- 681 Chen, Y.-C., Christensen, M. W., Xue, L., Sorooshian, A., Stephens, G. L., Rasmussen, R. M.
682 and Seinfeld, J. H.: Occurrence of lower cloud albedo in ship tracks, *Atmos. Chem. Phys.*,
683 12(17), 8223–8235, <https://doi.org/10.5194/acp-12-8223-2012>, 2012.
- 684 Chuang, C. C., Penner, J. E. and Edwards, L. L.: Nucleation Scavenging of Smoke Particles and
685 Simulated Drop Size Distributions over Large Biomass Fires, *J. Atmos. Sci.*, 49(14),
686 1264–1276, [https://doi.org/10.1175/1520-0469\(1992\)049<1264:NSOSPA>2.0.CO;2](https://doi.org/10.1175/1520-0469(1992)049<1264:NSOSPA>2.0.CO;2),
687 1992.
- 688 Chuang, C. C. and Penner, J. E.: Effects of anthropogenic sulfate on cloud drop nucleation and
689 optical properties, *Tellus B Chem. Phys. Meteorol.*, 47(5), 566–577,
690 <https://doi.org/10.1034/j.1600-0889.47.issue5.4.x>, 1995.
- 691 Coggon, M. M., Sorooshian, A., Wang, Z., Metcalf, A. R., Frossard, A. A., Lin, J. J., Craven, J.
692 S., Nenes, A., Jonsson, H. H., Russell, L. M., Flagan, R. C. and Seinfeld, J. H.: Ship
693 impacts on the marine atmosphere: Insights into the contribution of shipping emissions to
694 the properties of marine aerosol and clouds, *Atmos. Chem. Phys.*, 12(18), 8439–8458,
695 <https://doi.org/10.5194/acp-12-8439-2012>, 2012.
- 696 Coggon, M. M., Sorooshian, A., Wang, Z., Craven, J. S., Metcalf, A. R., Lin, J. J., Nenes, A.,
697 Jonsson, H. H., Flagan, R. C. and Seinfeld, J. H.: Observations of continental biogenic
698 impacts on marine aerosol and clouds off the coast of California, *J. Geophys. Res. Atmos.*,
699 119(11), 6724–6748, <https://doi.org/10.1002/2013JD021228>, 2014.
- 700 Crosbie, E., Wang, Z., Sorooshian, A., Chuang, P. Y., Craven, J. S., Coggon, M. M., Brunke, M.,
701 Zeng, X., Jonsson, H., Woods, R. K., Flagan, R. C. and Seinfeld, J. H.: Stratocumulus
702 Cloud Clearings and Notable Thermodynamic and Aerosol Contrasts across the Clear–
703 Cloudy Interface, *J. Atmos. Sci.*, 73(3), 1083–1099, <https://doi.org/10.1175/JAS-D-15-0137.1>, 2016.
- 705 Dadashazar, H., Wang, Z., Crosbie, E., Brunke, M., Zeng, X., Jonsson, H., Woods, R. K.,
706 Flagan, R. C., Seinfeld, J. H. and Sorooshian, A.: Relationships between giant sea salt
707 particles and clouds inferred from aircraft physicochemical data, *J. Geophys. Res.*, 122(6),
708 3421–3434, <https://doi.org/10.1002/2016JD026019>, 2017.
- 709 Dadashazar, H., Ma, L. and Sorooshian, A.: Sources of pollution and interrelationships between
710 aerosol and precipitation chemistry at a central California site, *Sci. Total Environ.*, 651,
711 1776–1787, <https://doi.org/10.1016/j.scitotenv.2018.10.086>, 2019.
- 712 Diamond, M. S., Dobracki, A., Freitag, S., Griswold, J. D. S., Heikkila, A., Howell, S. G.,
713 Kacarab, M. E., Podolske, J. R., Saide, P. E. and Wood, R.: Time-dependent entrainment
714 of smoke presents an observational challenge for assessing aerosol-cloud interactions over
715 the southeast Atlantic Ocean, *Atmos. Chem. Phys.*, 18(19), 14623–14636,
716 <https://doi.org/10.5194/acp-18-14623-2018>, 2018.
- 717 Facchini, M. C., Mircea, M., Fuzzi, S. and Charlson, R. J.: Cloud albedo enhancement by
718 surface-active organic solutes in growing droplets, *Nature*, 401(6750), 257–259,
719 <https://doi.org/10.1038/45758>, 1999.
- 720 Feingold, G., Frisch, A. S., Stevens, B. and Cotton, W. R.: On the relationship among cloud
721 turbulence, droplet formation and drizzle as viewed by Doppler radar, microwave
722 radiometer and lidar, *J. Geophys. Res. Atmos.*, 104(D18), 22195–22203,
723 <https://doi.org/10.1029/1999JD900482>, 1999.



- 724 Fountoukis, C. and Nenes, A.: Continued development of a cloud droplet formation
725 parameterization for global climate models, *J. Geophys. Res. Atmos.*, 110(D11), D11212,
726 <https://doi.org/10.1029/2004JD005591>, 2005.
- 727 Freund, R. J., Wilson, W. J. and Mohr, D. L.: *Statistical Methods*, 3rd ed., Academic Press,
728 Burlington, MA., 2010.
- 729 Gelaro, R., McCarty, W., Suárez, M. J., Todling, R., Molod, A., Takacs, L., Randles, C. A.,
730 Darmenov, A., Bosilovich, M. G., Reichle, R., Wargan, K., Coy, L., Cullather, R., Draper,
731 C., Akella, S., Buchard, V., Conaty, A., da Silva, A. M., Gu, W., Kim, G. K., Koster, R.,
732 Lucchesi, R., Merkova, D., Nielsen, J. E., Partyka, G., Pawson, S., Putman, W.,
733 Rienecker, M., Schubert, S. D., Sienkiewicz, M. and Zhao, B.: The modern-era
734 retrospective analysis for research and applications, version 2 (MERRA-2), *J. Clim.*,
735 30(14), 5419–5454, <https://doi.org/10.1175/JCLI-D-16-0758.1>, 2017.
- 736 Gerber, H., Arends, B. G. and Ackerman, A. S.: New microphysics sensor for aircraft use,
737 *Atmos. Res.*, 31(4), 235–252, [https://doi.org/10.1016/0169-8095\(94\)90001-9](https://doi.org/10.1016/0169-8095(94)90001-9), 1994.
- 738 Gerber, H., Frick, G. and Rodi, A. R.: Ground-based FSSP and PVM measurements of liquid
739 water content, *J. Atmos. Ocean. Technol.*, 16(8), 1143–1149,
740 [https://doi.org/10.1175/1520-0426\(1999\)016<1143:GBFAPM>2.0.CO;2](https://doi.org/10.1175/1520-0426(1999)016<1143:GBFAPM>2.0.CO;2), 1999.
- 741 Ghan, S. J., Leung, L. R. and Easter, R. C.: Prediction of cloud droplet number in a general
742 circulation model, *J. Geophys. Res.*, 102(D18), 21777–21794,
743 <https://doi.org/10.1029/97JD01810>, 1997.
- 744 Ghan, S. J., Abdul-Razzak, H., Nenes, A., Ming, Y., Liu, X., Ovchinnikov, M., Shipway, B.,
745 Meskhidze, N., Xu, J. and Shi, X.: Droplet nucleation: Physically-based parameterizations
746 and comparative evaluation, *J. Adv. Model. Earth Syst.*, 3(4), 1–34,
747 <https://doi.org/10.1029/2011ms000074>, 2011.
- 748 Grosvenor, D. P., Sourdeval, O., Zuidema, P., Ackerman, A., Alexandrov, M. D., Bennartz, R.,
749 Boers, R., Cairns, B., Chiu, J. C., Christensen, M., Deneke, H., Diamond, M., Feingold,
750 G., Fridlind, A., Hünerbein, A., Knist, C., Kollias, P., Marshak, A., McCoy, D., Merk, D.,
751 Painemal, D., Rausch, J., Rosenfeld, D., Russchenberg, H., Seifert, P., Sinclair, K., Stier,
752 P., van Dierenhoven, B., Wendisch, M., Werner, F., Wood, R., Zhang, Z. and Quaas, J.:
753 Remote Sensing of Droplet Number Concentration in Warm Clouds: A Review of the
754 Current State of Knowledge and Perspectives, *Rev. Geophys.*, 56(2), 409–453,
755 <https://doi.org/10.1029/2017RG000593>, 2018.
- 756 Hegg, D. A.: Impact of gas-phase HNO₃ and NH₃ on microphysical processes in atmospheric
757 clouds, *Geophys. Res. Lett.*, 27(15), 2201–2204, <https://doi.org/10.1029/1999GL011252>,
758 2000.
- 759 Hegg, D. A. and Hobbs, P. V.: Cloud Water Chemistry and the production of sulfates in clouds,
760 *Atmos. Environ.*, 15(9), 1597–1604, [https://doi.org/10.1016/0004-6981\(81\)90144-X](https://doi.org/10.1016/0004-6981(81)90144-X),
761 1981.
- 762 Hegg, D. A. and Hobbs, P. V.: Sulfate and nitrate chemistry in cumuliform clouds, *Atmos.*
763 *Environ.*, 20(5), 901–909, [https://doi.org/10.1016/0004-6981\(86\)90274-X](https://doi.org/10.1016/0004-6981(86)90274-X), 1986.
- 764 Hegg, D. A., Ferek, R. J. and Hobbs, P. V.: Light scattering and cloud condensation nucleus
765 activity of sulfate aerosol measured over the northeast Atlantic Ocean, *J. Geophys. Res.*
766 *Atmos.*, 98(D8), 14887–14894, <https://doi.org/10.1029/93JD01615>, 1993.
- 767 Hersey, S. P., Sorooshian, A., Murphy, S. M., Flagan, R. C. and Seinfeld, J. H.: Aerosol
768 hygroscopicity in the marine atmosphere: a closure study using high-resolution, size-



- 769 resolved AMS and multiple-RH DASH-SP data, *Atmos. Chem. Phys.*, 9(7), 16789–16817,
770 <https://doi.org/10.5194/acpd-8-16789-2008>, 2009.
- 771 Hudson, P. K., Murphy, D. M., Cziczo, D. J., Thomson, D. S., de Gouw, J. A., Warneke, C.,
772 Holloway, J., Jost, H. J. and Hübner, G.: Biomass-burning particle measurements:
773 Characteristics composition and chemical processing, *J. Geophys. Res. Atmos.*, 109,
774 D23S27, <https://doi.org/10.1029/2003JD004398>, 2004.
- 775 Intergovernmental Panel on Climate Change: *Climate Change 2007: The Physical Science Basis.*
776 *Contribution of Working Group I to the Fourth Assessment Report of the*
777 *Intergovernmental Panel on Climate Change*, Cambridge University Press, Cambridge,
778 United Kingdom and New York, NY, USA., 2007.
- 779 Intergovernmental Panel on Climate Change: *Climate Change 2013: The Physical Science Basis.*
780 *Contribution of Working Group I to the Fifth Assessment Report of the Intergovernmental*
781 *Panel on Climate Change*, Cambridge University Press, Cambridge, United Kingdom and
782 New York, NY, USA., 2013.
- 783 Jickells, T. D., An, Z. S., Andersen, K. K., Baker, A. R., Bergametti, G., Brooks, N., Cao, J. J.,
784 Boyd, P. W., Duce, R. A., Hunter, K. A., Kawahata, H., Kubilay, N. and Liss, P. S.:
785 Global Iron Connections Between Desert Dust, Ocean Biogeochemistry, and Climate,
786 *Science*, 308(5718), 67–71, <https://doi.org/10.1126/science.1105959>, 2005.
- 787 Kahane, L. H.: *Regression Basics*, 2nd ed., Sage Publications, Thousand Oaks, CA., 2008.
- 788 Koch, D. and Del Genio, A. D.: Black carbon semi-direct effects on cloud cover: Review and
789 synthesis, *Atmos. Chem. Phys.*, 10(16), 7685–7696, [https://doi.org/10.5194/acp-10-7685-](https://doi.org/10.5194/acp-10-7685-2010)
790 2010, 2010.
- 791 Kulmala, M., Laaksonen, A., Korhonen, P., Vesala, T., Ahonen, T. and Barrett, J. C.: The effect
792 of atmospheric nitric acid vapor on cloud condensation nucleus activation, *J. Geophys.*
793 *Res.*, 98(D12), 22949–22958, <https://doi.org/10.1029/93JD02070>, 1993.
- 794 Lance, S., Nenes, A., Mazzoleni, C., Dubey, M. K., Gates, H., Varutbangkul, V., Rissman, T. A.,
795 Murphy, S. M., Sorooshian, A., Flagan, R. C., Seinfeld, J. H., Feingold, G. and Jonsson,
796 H. H.: Cloud condensation nuclei activity, closure, and droplet growth kinetics of Houston
797 aerosol during the Gulf of Mexico Atmospheric Composition and Climate Study
798 (GoMACCS), *J. Geophys. Res.*, 114, D00F15, <https://doi.org/10.1029/2008jd011699>,
799 2009.
- 800 Leaitch, W. R., Strapp, J. W., Wiebe, H. A., Anlauf, K. G. and Isaac, G. A.: Chemical and
801 microphysical studies of nonprecipitating summer cloud in Ontario, Canada, *J. Geophys.*
802 *Res. Atmos.*, 91(D11), 11821–11831, <https://doi.org/10.1029/JD091iD11p11821>, 1986.
- 803 Leaitch, W. R., Isaac, G. A., Strapp, J. W., Banic, C. M. and Wiebe, H. A.: The relationship
804 between cloud droplet number concentrations and anthropogenic pollution: observations
805 and climatic implications, *J. Geophys. Res. Atmos.*, 97(D2), 2463–2474,
806 <https://doi.org/10.1029/91JD02739>, 1992.
- 807 Leaitch, W. R., Banic, C. M., Isaac, G. A., Couture, M. D., Liu, P. S. K., Gultepe, I., Li, S. M.,
808 Kleinman, L., Daum, P. H. and MacPherson, J. I.: Physical and chemical observations in
809 marine stratus during the 1993 North Atlantic Regional Experiment: Factors controlling
810 cloud droplet number concentrations, *J. Geophys. Res. Atmos.*, 101(D22), 29123–29135,
811 <https://doi.org/10.1029/96JD01228>, 1996.
- 812 Lowenthal, D. H. and Borys, R. D.: Sources of microphysical variation in marine stratiform
813 clouds in the North Atlantic, *Geophys. Res. Lett.*, 27(10), 1491–1494,
814 <https://doi.org/10.1029/1999GL010992>, 2000.



- 815 Lowenthal, D. H., Borys, R. D., Choulaton, T. W., Bower, K. N., Flynn, M. J. and Gallagher,
816 M. W.: Parameterization of the cloud droplet–sulfate relationship, *Atmos. Environ.*, 38(2),
817 287–292, <https://doi.org/10.1016/j.atmosenv.2003.09.046>, 2004.
- 818 Lu, M. L., Sorooshian, A., Jonsson, H. H., Feingold, G., Flagan, R. C. and Seinfeld, J. H.:
819 Marine stratocumulus aerosol-cloud relationships in the MASE-II experiment:
820 Precipitation susceptibility in eastern Pacific marine stratocumulus, *J. Geophys. Res.*
821 *Atmos.*, 114(24), 1–11, <https://doi.org/10.1029/2009JD012774>, 2009.
- 822 MacDonald, A. B., Dadashazar, H., Chuang, P. Y., Crosbie, E., Wang, H., Wang, Z., Jonsson, H.
823 H., Flagan, R. C., Seinfeld, J. H. and Sorooshian, A.: Characteristic Vertical Profiles of
824 Cloud Water Composition in Marine Stratocumulus Clouds and Relationships with
825 Precipitation, *J. Geophys. Res. Atmos.*, 123(7), 3704–3723,
826 <https://doi.org/10.1002/2017JD027900>, 2018.
- 827 Mardi, A. H., Dadashazar, H., MacDonald, A. B., Braun, R. A., Crosbie, E., Xian, P., Thorsen,
828 T. J., Coggon, M. M., Fenn, M. A., Ferrare, R. A., Hair, J. W., Woods, R. K., Jonsson, H.
829 H., Flagan, R. C., Seinfeld, J. H. and Sorooshian, A.: Biomass Burning Plumes in the
830 Vicinity of the California Coast: Airborne Characterization of Physicochemical Properties,
831 Heating Rates, and Spatiotemporal Features, *J. Geophys. Res. Atmos.*, 123(23), 13560–
832 13582, <https://doi.org/10.1029/2018JD029134>, 2018.
- 833 Mardi, A. H., Dadashazar, H., MacDonald, A. B., Crosbie, E., Coggon, M. M., Aghdam, M. A.,
834 Woods, R. K., Jonsson, H. H., Flagan, R. C., Seinfeld, J. H. and Sorooshian, A.: Effects of
835 Biomass Burning on Stratocumulus Droplet Characteristics, Drizzle Rate, and
836 Composition, *J. Geophys. Res. Atmos.*, 124(22), 12301–12318,
837 <https://doi.org/10.1029/2019JD031159>, 2019.
- 838 Matsumoto, K., Tanaka, H., Nagao, I. and Ishizaka, Y.: Contribution of particulate sulfate and
839 organic carbon to cloud condensation nuclei in the marine atmosphere, *Geophys. Res.*
840 *Let.*, 24(6), 655–658, <https://doi.org/10.1029/97GL00541>, 1997.
- 841 Maudlin, L. C., Wang, Z., Jonsson, H. H. and Sorooshian, A.: Impact of wildfires on size-
842 resolved aerosol composition at a coastal California site, *Atmos. Environ.*, 119, 59–68,
843 <https://doi.org/10.1016/j.atmosenv.2015.08.039>, 2015.
- 844 McCoy, D. T., Bender, F. A.-M., Mohrmann, J. K. C., Hartmann, D. L., Wood, R. and
845 Grosvenor, D. P.: The global aerosol-cloud first indirect effect estimated using MODIS,
846 MERRA, and AeroCom, *J. Geophys. Res. Atmos.*, 122(3), 1779–1796,
847 <https://doi.org/10.1002/2016JD026141>, 2017.
- 848 McCoy, D. T., Bender, F. A.-M., Grosvenor, D. P., Mohrmann, J. K., Hartmann, D. L., Wood, R.
849 and Field, P. R.: Predicting decadal trends in cloud droplet number concentration using
850 reanalysis and satellite data, *Atmos. Chem. Phys.*, 18(3), 2035–2047,
851 <https://doi.org/10.5194/acp-18-2035-2018>, 2018.
- 852 Medina, J., Nenes, A., Sotiropoulou, R. E. P., Cottrell, L. D., Ziemba, L. D., Beckman, P. J. and
853 Griffin, R. J.: Cloud condensation nuclei closure during the International Consortium for
854 Atmospheric Research on Transport and Transformation 2004 campaign: Effects of size-
855 resolved composition, *J. Geophys. Res. Atmos.*, 112(D10), D10S31,
856 <https://doi.org/10.1029/2006JD007588>, 2007.
- 857 Menon, S. and Saxena, V. K.: Role of sulfates in regional cloud–climate interactions, *Atmos.*
858 *Res.*, 47–48, 299–315, [https://doi.org/https://doi.org/10.1016/S0169-8095\(98\)00057-X](https://doi.org/https://doi.org/10.1016/S0169-8095(98)00057-X),
859 1998.



- 860 Menon, S., Genio, A. D. Del, Koch, D. and Tselioudis, G.: GCM Simulations of the Aerosol
861 Indirect Effect: Sensitivity to Cloud Parameterization and Aerosol Burden, *J. Atmos. Sci.*,
862 59(3), 692–713, [https://doi.org/10.1175/1520-0469\(2002\)059<0692:gsotai>2.0.co;2](https://doi.org/10.1175/1520-0469(2002)059<0692:gsotai>2.0.co;2),
863 2002.
- 864 Nenes, A., Charlson, R. J., Facchini, M. C., Kulmala, M., Laaksonen, A. and Seinfeld, J. H.: Can
865 chemical effects on cloud droplet number rival the first indirect effect?, *Geophys. Res.*
866 *Lett.*, 29(17), 1848, <https://doi.org/10.1029/2002gl015295>, 2002.
- 867 Nenes, A. and Seinfeld, J. H.: Parameterization of cloud droplet formation in global climate
868 models, *J. Geophys. Res. Atmos.*, 108(D14), 1–14, <https://doi.org/10.1029/2002jd002911>,
869 2003.
- 870 Novakov, T. and Penner, J. E.: Large contribution of organic aerosols to cloud-condensation-
871 nuclei concentrations, *Nature*, 365(6449), 823–826, <https://doi.org/10.1038/365823a0>,
872 1993.
- 873 Novakov, T., Rivera-Carpio, C., Penner, J. E. and Rogers, C. F.: The effect of anthropogenic
874 sulfate aerosols on marine cloud droplet concentrations, *Tellus B Chem. Phys. Meteorol.*,
875 46(2), 132–141, <https://doi.org/10.3402/tellusb.v46i2.15758>, 1994.
- 876 Partridge, D. G., Vrugt, J. A., Tunved, P., Ekman, A. M. L., Struthers, H. and Sorooshian, A.:
877 Inverse modelling of cloud-aerosol interactions - Part 2: Sensitivity tests on liquid phase
878 clouds using a Markov chain Monte Carlo based simulation approach, *Atmos. Chem.*
879 *Phys.*, 12(6), 2823–2847, <https://doi.org/10.5194/acp-12-2823-2012>, 2012.
- 880 Paulot, F., Jacob, D. J., Johnson, M. T., Bell, T. G., Baker, A. R., Keene, W. C., Lima, I. D.,
881 Doney, S. C. and Stock, C. A.: Global oceanic emission of ammonia: Constraints from
882 seawater and atmospheric observations, *Global Biogeochem. Cycles*, 29(8), 1165–1178,
883 <https://doi.org/10.1002/2015GB005106>, 2015.
- 884 Prabhakar, G., Ervens, B., Wang, Z., Maudlin, L. C., Coggon, M. M., Jonsson, H. H., Seinfeld, J.
885 H. and Sorooshian, A.: Sources of nitrate in stratocumulus cloud water: Airborne
886 measurements during the 2011 E-PEACE and 2013 NiCE studies, *Atmos. Environ.*, 97,
887 166–173, <https://doi.org/10.1016/j.atmosenv.2014.08.019>, 2014.
- 888 Pringle, K. J., Carslaw, K. S., Spracklen, D. V., Mann, G. M. and Chipperfield, M. P.: The
889 relationship between aerosol and cloud drop number concentrations in a global aerosol
890 microphysics model, *Atmos. Chem. Phys.*, 9(12), 4131–4144, [https://doi.org/10.5194/acp-](https://doi.org/10.5194/acp-9-4131-2009)
891 [9-4131-2009](https://doi.org/10.5194/acp-9-4131-2009), 2009.
- 892 Pueschel, R. F., Valin, C. C., Castillo, R. C., Kadlecck, J. A. and Ganor, E.: Aerosols in polluted
893 versus nonpolluted air masses: long-range transport and effects on clouds, *J. Appl.*
894 *Meteorol. Clim.*, 25, 1908–1917, [https://doi.org/10.1175/1520-](https://doi.org/10.1175/1520-0450(1986)025<1908:AIPVNA>2.0.CO;2)
895 [0450\(1986\)025<1908:AIPVNA>2.0.CO;2](https://doi.org/10.1175/1520-0450(1986)025<1908:AIPVNA>2.0.CO;2), 1986.
- 896 Quinn, P. K., Coffman, D. J., Johnson, J. E., Upchurch, L. M. and Bates, T. S.: Small fraction of
897 marine cloud condensation nuclei made up of sea spray aerosol, *Nat. Geosci.*, 10(9), 674–
898 679, <https://doi.org/10.1038/ngeo3003>, 2017.
- 899 Reid, J. S., Hobbs, P. V., Ferek, R. J., Blake, D. R., Martins, J. V., Dunlap, M. R. and Liousse,
900 C.: Physical, chemical, and optical properties of regional hazes dominated by smoke in
901 Brazil, *J. Geophys. Res. Atmos.*, 103(D24), 32059–32080,
902 <https://doi.org/10.1029/98JD00458>, 1998.
- 903 Russell, L. M., Sorooshian, A., Seinfeld, J. H., Albrecht, B. A., Nenes, A., Ahlm, L., Chen, Y.-
904 C., Coggon, M., Craven, J. S., Flagan, R. C., Frossard, A. A., Jonsson, H., Jung, E., Lin, J.
905 J., Metcalf, A. R., Modini, R., Mülmenstädt, J., Roberts, G. C., Shingler, T., Song, S.,



- 906 Wang, Z. and Wonaschütz, A.: Eastern pacific emitted aerosol cloud experiment, *Bull.*
907 *Am. Meteorol. Soc.*, 94(5), 709–729, <https://doi.org/10.1175/BAMS-D-12-00015.1>, 2013.
- 908 Saxena, V. K. and Menon, S.: Sulfate-induced cooling in the southeastern US: An observational
909 assessment, *Geophys. Res. Lett.*, 26(16), 2489–2492,
910 <https://doi.org/10.1029/1999GL900555>, 1999.
- 911 Schlosser, J. S., Braun, R. A., Bradley, T., Dadashazar, H., MacDonald, A. B., Aldhaif, A. A.,
912 Azadi Aghdam, M., Hossein Mardi, A., Xian, P. and Sorooshian, A.: Analysis of Aerosol
913 Composition Data for Western United States Wildfires Between 2005-2015: Dust
914 Emissions, Chloride Depletion, and Most Enhanced Aerosol Constituents, *J. Geophys.*
915 *Res. Atmos.*, 122(16), 8951–8966, <https://doi.org/10.1002/2017JD026547>, 2017.
- 916 Seinfeld, J. H. and Pandis, S. N.: *Atmospheric Chemistry and Physics*, 3rd ed., New York, NY.,
917 2016.
- 918 Silva, P. J., Liu, D. Y., Noble, C. A. and Prather, K. A.: Size and chemical characterization of
919 individual particles resulting from biomass burning of local Southern California species,
920 *Environ. Sci. Technol.*, 33(18), 3068–3076, <https://doi.org/10.1021/es980544p>, 1999.
- 921 Sorooshian, A., Lu, M. L., Brechtel, F. J., Jonsson, H., Feingold, G., Flagan, R. C. and Seinfeld,
922 J. H.: On the source of organic acid aerosol layers above clouds, *Environ. Sci. Technol.*,
923 41(13), 4647–4654, <https://doi.org/10.1021/es0630442>, 2007.
- 924 Sorooshian, A., Padró, L. T., Nenes, A., Feingold, G., McComiskey, A., Hersey, S. P., Gates, H.,
925 Jonsson, H. H., Miller, S. D., Stephens, G. L., Flagan, R. C. and Seinfeld, J. H.: On the
926 link between ocean biota emissions, aerosol, and maritime clouds: Airborne, ground, and
927 satellite measurements off the coast of California, *Global Biogeochem. Cycles*, 23(4), 1–
928 15, <https://doi.org/10.1029/2009GB003464>, 2009.
- 929 Sorooshian, A., MacDonald, A. B., Dadashazar, H., Bates, K. H., Coggon, M. M., Craven, J. S.,
930 Crosbie, E., Hersey, S. P., Hodas, N., Lin, J. J., Negrón Marty, A., Maudlin, L. C.,
931 Metcalf, A. R., Murphy, S. M., Padró, L. T., Prabhakar, G., Rissman, T. A., Shingler, T.,
932 Varutbangkul, V., Wang, Z., Woods, R. K., Chuang, P. Y., Nenes, A., Jonsson, H. H.,
933 Flagan, R. C. and Seinfeld, J. H.: A multi-year data set on aerosol-cloud-precipitation-
934 meteorology interactions for marine stratocumulus clouds, *Sci. Data*, 5, 1–13,
935 <https://doi.org/10.1038/sdata.2018.26>, 2018.
- 936 Sorooshian, A., Anderson, B., Bauer, S. E., Braun, R. A., Cairns, B., Crosbie, E., Dadashazar,
937 H., Diskin, G., Ferrare, R., Flagan, R. C., Hair, J., Hostetler, C., Jonsson, H. H., Kleb, M.
938 M., Liu, H., Macdonald, A. B., McComiskey, A., Moore, R., Painemal, D., Russell, L. M.,
939 Seinfeld, J. H., Shook, M., Smith, W. L., Thornhill, K., Tselioudis, G., Wang, H., Zeng,
940 X., Zhang, B., Ziemba, L. and Zuidema, P.: Aerosol–cloud–meteorology interaction
941 airborne field investigations: Using lessons learned from the U.S. West coast in the design
942 of activate off the U.S. East Coast, *Bull. Am. Meteorol. Soc.*, 100(8), 1511–1528,
943 <https://doi.org/10.1175/BAMS-D-18-0100.1>, 2019.
- 944 Sorooshian, A., Corral, A. F., Braun, R. A., Cairns, B., Crosbie, E., Ferrare, R., Hair, J., Kleb, M.
945 M., Hossein Mardi, A., Maring, H., McComiskey, A., Moore, R., Painemal, D., Scarino,
946 A. J., Schlosser, J., Shingler, T., Shook, M., Wang, H., Zeng, X., Ziemba, L. and Zuidema,
947 P.: Atmospheric Research Over the Western North Atlantic Ocean Region and North
948 American East Coast: A Review of Past Work and Challenges Ahead, *J. Geophys. Res.*
949 *Atmos.*, in press, <https://doi.org/10.1029/2019JD031626>, 2020.
- 950 Strapp, J. W., Leaitch, W. R. and Liu, P. S. K.: Hydrated and dried aerosol-size-distribution
951 measurements from the Particle Measuring Systems FSSP-300 probe and the deiced



- 952 PCASP-100X probe, *J. Atmos. Ocean. Technol.*, 9(5), 548–555,
953 [https://doi.org/10.1175/1520-0426\(1992\)009<0548:HADASD>2.0.CO;2](https://doi.org/10.1175/1520-0426(1992)009<0548:HADASD>2.0.CO;2), 1992.
- 954 Twomey, S.: The nuclei of natural cloud formation part II: The supersaturation in natural clouds
955 and the variation of cloud droplet concentration, *Geofis. Pura e Appl.*, 43(1), 243–249,
956 <https://doi.org/10.1007/BF01993560>, 1959.
- 957 Twomey, S.: The influence of pollution on the shortwave albedo of clouds, *J. Atmos. Sci.*, 34,
958 1149–1152, [https://doi.org/10.1175/1520-0469\(1977\)034<1149:TIOPO>2.0.CO;2](https://doi.org/10.1175/1520-0469(1977)034<1149:TIOPO>2.0.CO;2), 1977.
- 959 Van Dingenen, R., Raes, F. and Jensen, N. R.: Evidence for anthropogenic impact on number
960 concentration and sulfate content of cloud-processed aerosol particles over the North
961 Atlantic, *J. Geophys. Res. Atmos.*, 100(D10), 21057–21067,
962 <https://doi.org/10.1029/95jd02141>, 1995.
- 963 Wang, Z., Sorooshian, A., Prabhakar, G., Coggon, M. M. and Jonsson, H. H.: Impact of
964 emissions from shipping, land, and the ocean on stratocumulus cloud water elemental
965 composition during the 2011 E-PEACE field campaign, *Atmos. Environ.*, 89, 570–580,
966 <https://doi.org/10.1016/j.atmosenv.2014.01.020>, 2014.
- 967 Wang, Z., Mora Ramirez, M., Dadashazar, H., MacDonald, A. B., Crosbie, E., Bates, K. H.,
968 Coggon, M. M., Craven, J. S., Lynch, P., Campbell, J. R., Azadi Aghdam, M., Woods, R.
969 K., Jonsson, H., Flagan, R. C., Seinfeld, J. H. and Sorooshian, A.: Contrasting cloud
970 composition between coupled and decoupled marine boundary layer clouds, *J. Geophys.
971 Res. Atmos.*, 121(19), 11679–11691, <https://doi.org/10.1002/2016JD025695>, 2016.
- 972 West, R. E. L., Stier, P., Jones, A., Johnson, C. E., Mann, G. W., Bellouin, N., Partridge, D. G.
973 and Kipling, Z.: The importance of vertical velocity variability for estimates of the
974 indirect aerosol effects, *Atmos. Chem. Phys.*, 14(12), 6369–6393,
975 <https://doi.org/10.5194/acp-14-6369-2014>, 2014.
- 976 Wonaschütz, A., Coggon, M., Sorooshian, A., Modini, R., Frossard, A. A., Ahlm, L.,
977 Mülmenstädt, J., Roberts, G. C., Russell, L. M., Dey, S., Brechtel, F. J. and Seinfeld, J. H.:
978 Hygroscopic properties of smoke-generated organic aerosol particles emitted in the marine
979 atmosphere, *Atmos. Chem. Phys.*, 13(19), 9819–9835, <https://doi.org/10.5194/acp-13-9819-2013>, 2013.
- 981 Xue, H. and Feingold, G.: A modeling study of the effect of nitric acid on cloud properties, *J.
982 Geophys. Res.*, 109, D18204, <https://doi.org/10.1029/2004JD004750>, 2004.
- 983
984



985 **Table 1.** Summary of field campaign data sets used in this study and statistics related to cloud
986 water sample collection. Smoke-influenced RFs were NiCE RFs 16—23 and FASE RFs 3—11
987 and 13—15.

Field campaign	Dates (mm/dd/yyyy)	# of RFs	# of samples	# of fire-impacted samples
Eastern Pacific Emitted Aerosol Cloud Experiment (E-PEACE)	07/08/2011 – 08/18/2011	30	82	0
Nucleation in California Experiment (NiCE)	07/08/2013 – 08/07/2013	23	119	31
Biological and Oceanic Atmospheric Study (BOAS)	07/02/2015 – 07/24/2015	15	29	0
Fog and Stratocumulus Evolution Experiment (FASE)	07/18/2016 – 08/12/2016	16	155	136

988
989
990
991



992 **Table 2.** Summary of chemical species analyzed in this study. IC = ion chromatography; ICP =
 993 ICP-MS or ICP-QQQ. Note: NSS species, with the exception of NSS-SO₄²⁻, were calculated
 994 using elements, not ions, hence they have no superscript charge.

Elements (ICP)		Inorganic ions (IC)	Organic ions (IC)
1 Ag	24 Na	47 Ammonium (NH ₄ ⁺)	66 Acetate
2 Al	25 Nb	48 Bromide (Br ⁻)	67 Adipate
3 As	26 Ni	49 Calcium (Ca ²⁺)	68 Butyrate
4 B	27 P	50 Chloride (Cl ⁻)	69 Formate
5 Ba	28 Pb	51 Fluoride (F ⁻)	70 Glutarate
6 Br	29 Pd	52 Lithium (Li ⁺)	71 Glycolate
7 C	30 Rb	53 Magnesium (Mg ²⁺)	72 Glyoxylate
8 Ca	31 Rh	54 Methanesulfonic acid (MSA)	73 Lactate
9 Cd	32 Ru	55 Nitrate (NO ₃ ⁻)	74 Maleate
10 Cl	33 S	56 Nitrite (NO ₂ ⁻)	75 Malonate
11 Co	34 Sb	57 Potassium (K ⁺)	76 Oxalate
12 Cr	35 Se	58 Sodium (Na ⁺)	77 Propionate
13 Cs	36 Si	59 Sulfate (SO ₄ ²⁻)	78 Pyruvate
14 Cu	37 Sn		79 Succinate
15 Fe	38 Sr	<u>Amines (IC)</u>	
16 Ga	39 Ta	60 Diethyl ammonium (DEA)	
17 Hf	40 Te	61 Dimethyl ammonium (DMA)	
18 I	41 Ti		
19 K	42 V	<u>NSS species (calculated)</u>	
20 Li	43 W	62 NSS Calcium (NSS-Ca)	
21 Mg	44 Y	63 NSS Potassium (NSS-K)	
22 Mn	45 Zn	64 NSS Magnesium (NSS-Mg)	
23 Mo	46 Zr	65 NSS Sulfate (NSS-SO ₄ ²⁻)	

995
 996
 997
 998
 999



1000 **Table 3.** Summary of one-predictor models for N_d based on using any of nine of the final
1001 chemical species that were identified after applying the filtering scheme shown in Figure 2. The
1002 coefficients correspond to a linear model of the form $\log(N_d) = a_0 + a_1 \log(M_i)$, where M_i is the
1003 mass concentration of species i .

Species	R^2_{adj}	Coefficients	
		a_0	a_1
Tot-SO ₄ ²⁻	0.40	2.05	0.32
NH ₄ ⁺	0.34	2.33	0.25
NSS-SO ₄ ²⁻	0.29	2.13	0.28
MSA	0.26	2.37	0.31
NO ₃ ⁻	0.24	2.12	0.25
Na	0.19	2.03	0.13
Ox	0.15	2.26	0.18
V	0.14	2.61	0.15
Fe	0.05	2.26	0.09

1004



1005 **Table 4.** Comparison of coefficient values for studies that correlate N_d to SO_4^{2-} (total or non-sea
 1006 salt). The coefficients correspond to a linear model of the form $\log(N_d) = a_0 + a_1 \log(\text{SO}_4^{2-})$.

Reference	a_0	a_1	SO_4^{2-}	R^2	Cloud type
Leitch et al. (1992) ^a	1.95	0.257	Tot	0.3	Stratocumulus
	2.33	0.186	Tot	0.49	Cumulus
Novakov et al. (1994)	2.323	0.091	NSS	0.50 ^b	Marine stratocumulus
	2.43	-0.056	NSS	0.03	Marine cumulus
Van Dingenen et al. (1995) ^c	2.33	0.4	NSS	0.42	All cloud types combined
	2.24	0.257	NSS	^d	Continental stratus
	2.54	0.186	NSS	^d	Continental cumulus
Boucher & Lohmann (1995) ^c	2.06	0.48	NSS	^d	Marine
	2.21	0.41	NSS	^d	All cloud types combined
Saxena & Menon (1999)	0.67	0.66	Tot	^d	Continental orographic clouds
	2.32	0.74	NSS	0.82	Marine
Lowenthal et al. (2004)	2.38	0.49	NSS	0.66	Continental
	2.39	0.5	NSS	0.81	Combined
McCoy et al. (2017)	2.11	0.41	NSS	0.36	Marine stratocumulus

^a The units of SO_4^{2-} for this regression are nEq m^{-3} . All other studies report SO_4^{2-} in units of $\mu\text{g m}^{-3}$.

However, the value of a_1 is not affected by the units of concentration.

^b The R^2 has a $p > 0.05$ due to having few data points.

^c These regressions were made using data compiled from several studies and assume that $N_{\text{CCN}} \sim N_d$.

^d Study does not report R^2 .

1007
 1008



1009 **Table 5.** The top three statistically significant regressions with the highest R^2_{adj} for a given
 1010 number of predictors. The coefficients correspond to a linear model of the form $\log(N_d) = a_0 + \sum$
 1011 $a_i \log(P_i)$.
 1012

# of Predictors	Predictors (P_i) and their respective coefficients (a_i)											R^2_{adj}
	a_0	a_1	P_1	a_2	P_2	a_3	P_3	a_4	P_4	a_5	P_5	
1	2.05	0.32	Tot-SO ₄ ²⁻									0.40
	2.33	0.25	NH ₄ ⁺									0.34
	2.13	0.28	NSS-SO ₄ ²⁻									0.29
2	2.18	0.22	Tot-SO ₄ ²⁻	0.12	NH ₄ ⁺							0.48
	2.43	0.21	MSA	0.15	NH ₄ ⁺							0.44
	2.25	0.19	NH ₄ ⁺	0.09	Na							0.42
3	2.25	0.13	NSS-SO ₄ ²⁻	0.13	NH ₄ ⁺	0.10	Na					0.50
	2.24	0.19	Tot-SO ₄ ²⁻	0.10	Ox	0.07	NH ₄ ⁺					0.49
	2.25	0.17	Tot-SO ₄ ²⁻	0.11	NH ₄ ⁺	0.08	MSA					0.49
4	2.32	0.21	Tot-SO ₄ ²⁻	0.20	Ox	0.09	NH ₄ ⁺	-0.15	NO ₃ ⁻			0.52
	2.29	0.11	NSS-SO ₄ ²⁻	0.10	Ox	0.09	Na	0.08	NH ₄ ⁺			0.51
	2.31	0.11	NH ₄ ⁺	0.10	NSS	0.10	MSA	0.08	Na			0.51
5	2.10	0.13	Na	0.12	Ox	0.11	NSS-SO ₄ ²⁻	0.08	NH ₄ ⁺	-0.05	V	0.56
	2.40	0.23	Ox	0.13	NSS-SO ₄ ²⁻	0.10	NH ₄ ⁺	0.09	Na	-0.17	NO ₃ ⁻	0.55
	2.36	0.14	NH ₄ ⁺	0.14	MSA	0.12	NSS-SO ₄ ²⁻	0.07	Na	-0.08	NO ₃ ⁻	0.52

1013
 1014



1015 **Table 6.** Comparison of regressions containing NSS-SO₄²⁻, Na, and Ox.

# of Predictors	Predictors (P _i) and their respective coefficients (a _i)							R ² _{adj}
	a ₀	a ₁	P ₁	a ₂	P ₂	a ₃	P ₃	
1	2.13	0.28	NSS-SO ₄ ²⁻					0.29
2	2.12	0.23	NSS-SO ₄ ²⁻	0.12	Na			0.40
	2.26	0.24	NSS-SO ₄ ²⁻	0.12	Ox			0.34
3	2.22	0.22	NSS-SO ₄ ²⁻	0.10	Na	0.08	Ox	0.42

1016
1017
1018



1019 **Table 7.** Results of multivariable regressions from previous studies that have correlated N_d to
 1020 mass concentrations. The regression corresponds to a model like Equation 3.

Reference	Predictors (P_i) and their respective coefficients (a_i)								R^2	Cloud type	
	a_0	a_1	P_1	a_2	P_2	a_3	P_3	a_4			P_4
Menon et al. (2002) ^a	2.41	0.50	NSS-SO ₄ ²⁻	0.13	OM ^b						Continental
	2.41	0.50	NSS-SO ₄ ²⁻	0.13	OM	0.05	SS				Marine
McCoy et al. (2017)	1.78	0.31	NSS-SO ₄ ²⁻	-0.19	SS	0.057	BC	0.031	DU	0.44	Marine stratocumulus (global average)
McCoy et al. (2018)	2.03	0.2	NSS-SO ₄ ²⁻	-0.04	SS	-0.03	BC	0	DU	0.08	Marine stratocumulus (just Californian coast)

^a This study obtains data from other studies and calculates organic matter.

^b OM = Organic Matter, SS = Sea Salt, BC = Black Carbon, DU = Dust.

1021
 1022
 1023

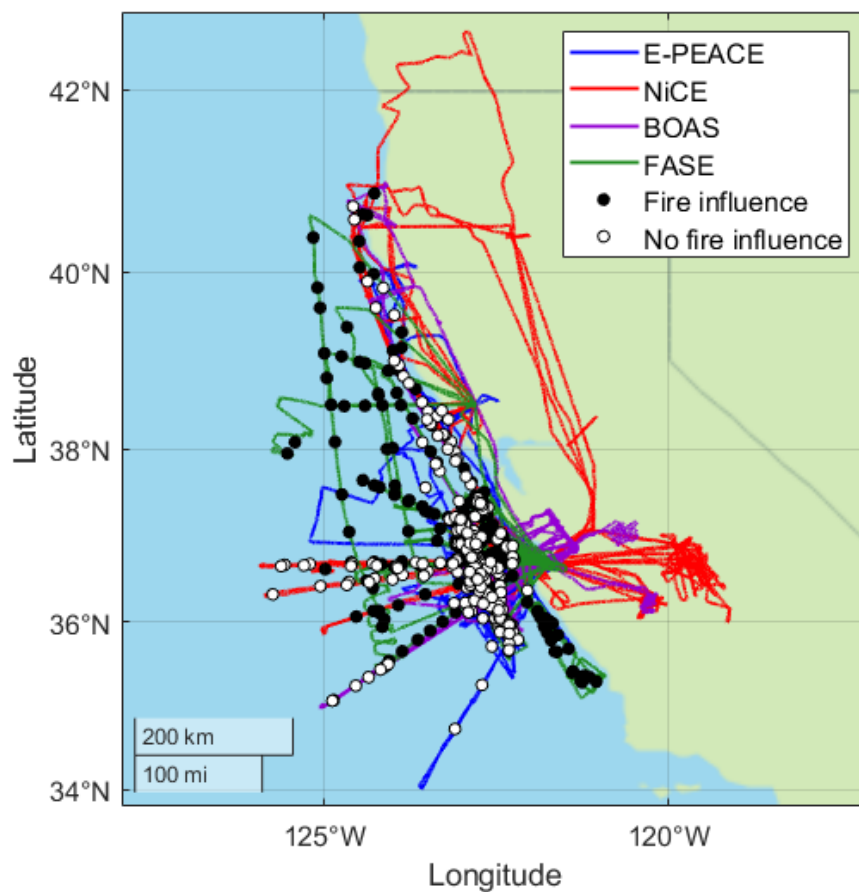


1024 **Table 8.** Summary of the R^2_{adj} obtained when correlating mass concentration of a species to N_d
1025 under different atmospheric conditions.

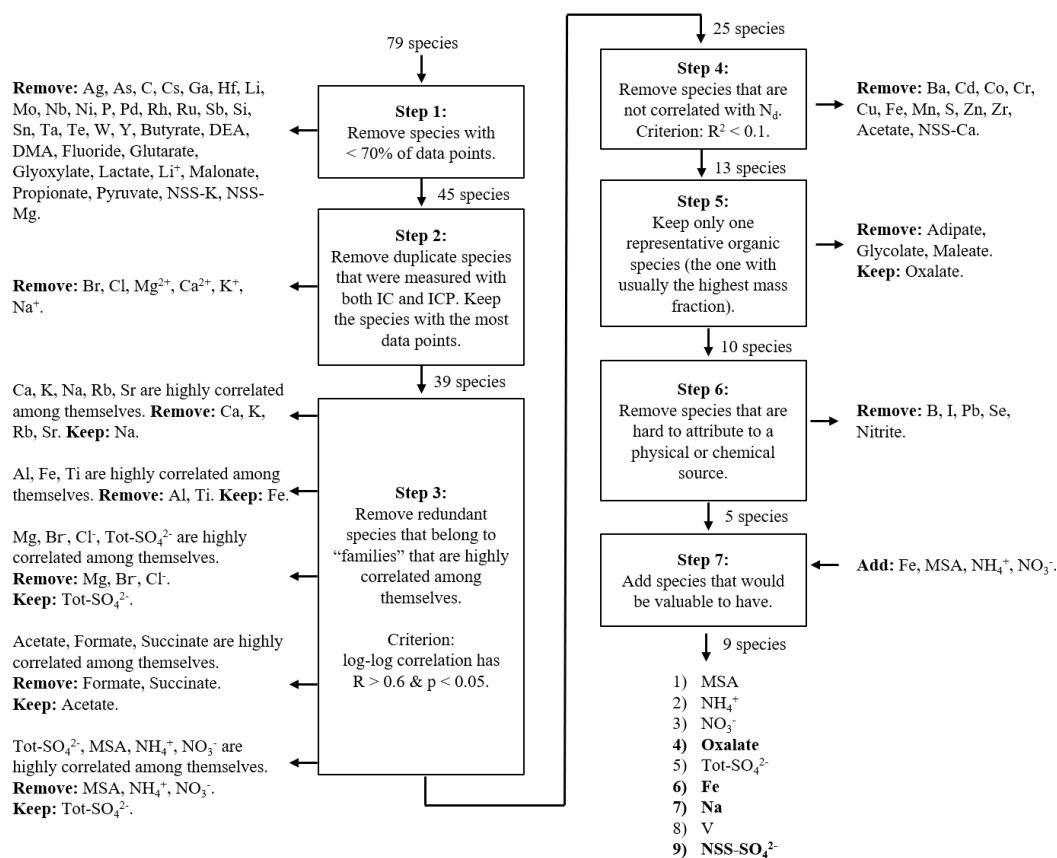
Binning criterion	Data points considered	R^2_{adj}			
		NSS-SO ₄ ²⁻	Na	Ox	Fe
None	All	0.29	0.19	0.15	0.05
Turbulence	High σ_w	0.27	0.26	0.09	0.02 ^a
	Low σ_w	0.27	0.09	0.30	0.07
Smoke influence	Smoke	0.22	0.17	0.42	0.15
	No smoke	0.36	0.24	0.07	0.04
Normalized cloud height	Top third	0.33	0.33	0.08	0.03
	Middle third	0.29	0.16	0.16	0.03
	Bottom third	0.17	0.10	0.29	0.20

^a This R^2_{adj} has a p-value > 0.05.

1026
1027
1028
1029
1030

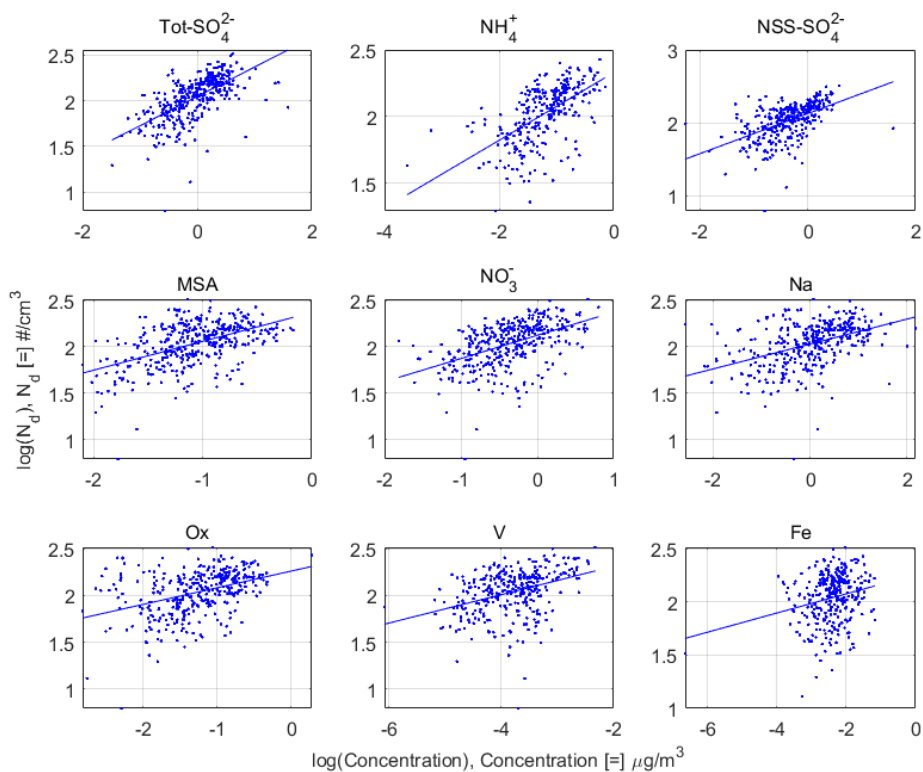


1031
1032 **Figure 1.** Flight paths for each of the four campaigns used in this study. Markers indicate the
1033 average location at which the cloud water samples were collected. Smoke- and non-smoke-
1034 influenced samples are indicated with filled and open markers, respectively.
1035
1036
1037



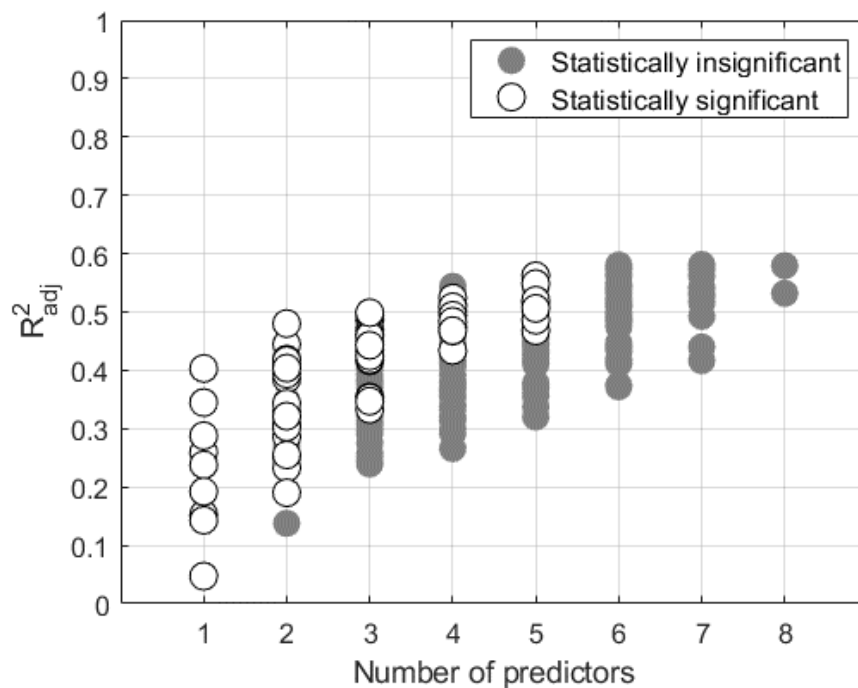
1038
 1039
 1040
 1041
 1042
 1043

Figure 2. Algorithm used to filter the number of species from 79 to 9. The four bolded species are the ones used in Section 3.3). ICP = ICP-MS + ICP-QQQ.



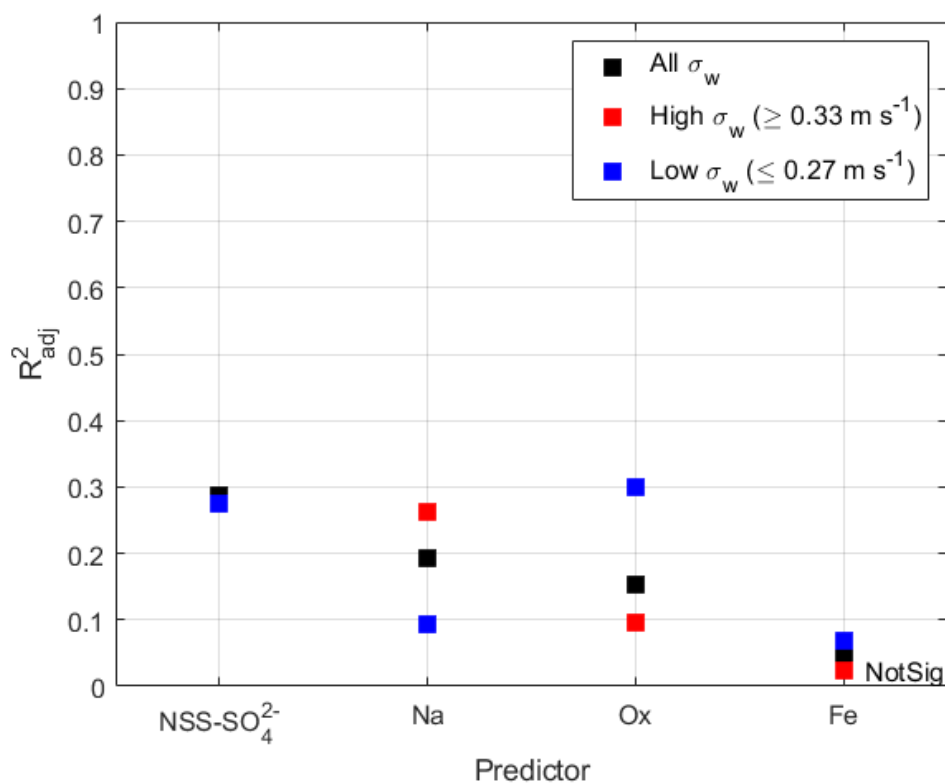
1044
1045
1046
1047
1048

Figure 3. Scatter plot for the nine filtered species from Figure 2. The lines are linear regression models of the form $\log(N_d) = a_0 + a_1 \log(M_i)$, where M_i is the mass concentration of species i .

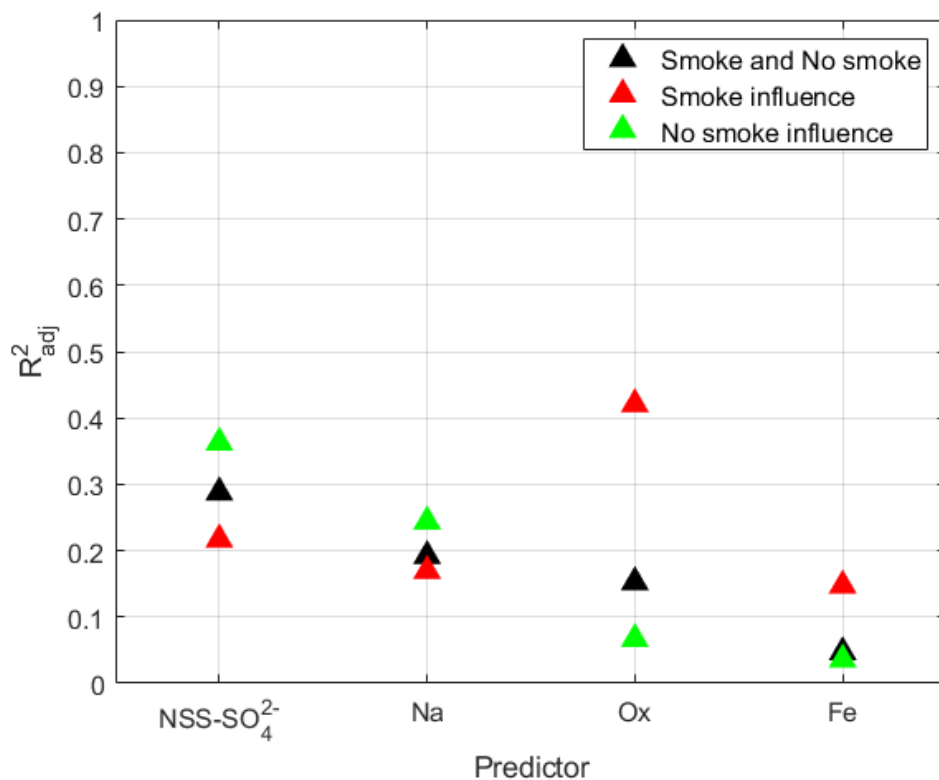


1049
1050
1051
1052
1053
1054

Figure 4. Plot showing which of the 383 regressions are statistically significant. This plot ignores the regressions that use both NSS-SO_4^{2-} and Tot-SO_4^{2-} simultaneously.

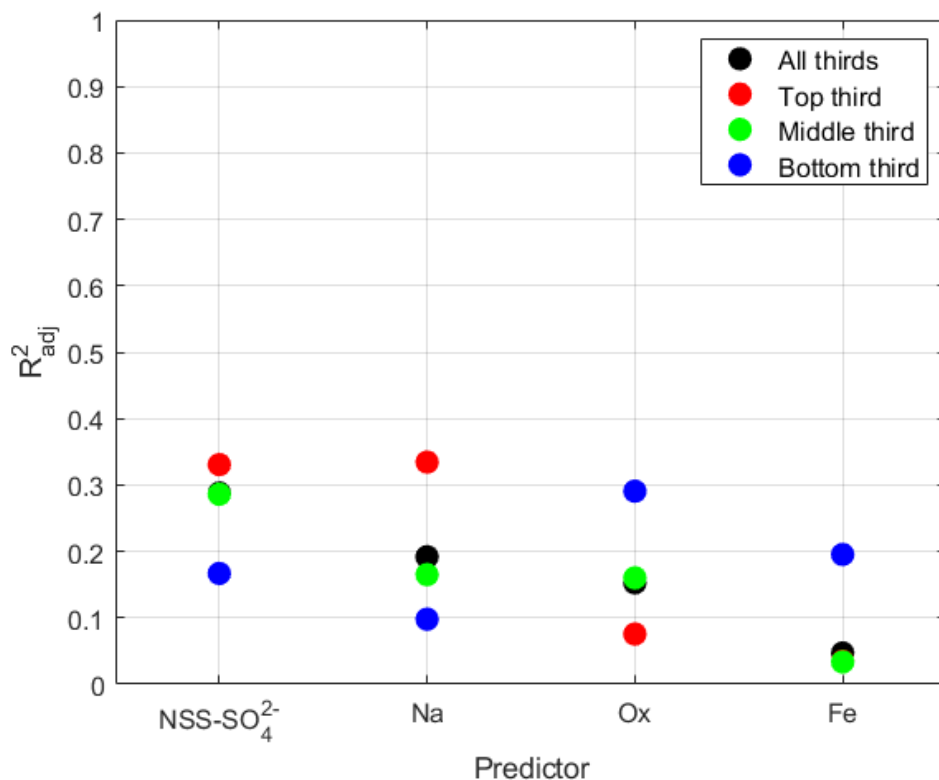


1055
1056 **Figure 5.** Effect of turbulence (quantified using σ_w) on the ability of a single species to predict
1057 N_d . For NSS-SO₄²⁻, the high (red) and low (blue) σ_w data points overlap. NotSig = Not
1058 statistically significant according to the definition in Section 2.5.
1059
1060
1061



1062
1063
1064
1065
1066

Figure 6. Effect of the influence of smoke on the ability of a single species to predict N_d .



1067
1068
1069
1070
1071
1072
1073

Figure 7. Effect of the influence of normalized cloud height on the ability of a single species to predict N_d . For Fe, the top 3rd (red) data point overlaps with the middle and bottom 3rd (green and blue) data points.